Abscinazole-F1, a conformationally restricted analogue of the plant growth retardant uniconazole and an inhibitor of ABA 8'-hydroxylase CYP707A with no growth-retardant effect

Yasushi Todoroki,[a,*] Kyotaro Kobayashi,[a] Minaho Shirakura,[a] Hikaru Aoyama,[a] Kokichi Takatori,[a] Hataitip Nimitkeatkai,[b] Mei-Hong Jin,[a] Saori Hiramatsu,[a] Kotomi Ueno,[c,†] Satoru Kondo,[b] Masaharu Mizutani,[d,‡] Nobuhiro Hirai[e]

[a] *Department of Applied Biological Chemistry, Faculty of Agriculture, Shizuoka University, Shizuoka 422-8529, Japan*
[b] *Division of Bioresource Science, Graduate School of Horticulture, Chiba University, Matsudo 271-8510, Japan*
[c] *The United Graduate School of Agricultural Science, Gifu University, Gifu 501-1193, Japan*
[d] *Institute for Chemical Research, Kyoto University, Uji, Kyoto 611-0011, Japan*
[e] *Division of Environmental Science and Technology, Graduate School of Agriculture, Kyoto University, Kyoto 606-8501, Japan*

* Corresponding author.   Phone&Fax: +81-54-238-4871.   E-mail: aytodor@agr.shizuoka.ac.jp

† Present address: Graduate School of Agricultural and Life Sciences, The University of Tokyo, Tokyo 113-8657, Japan.

‡ Present address: Graduate School of Agricultural Science, Kobe University, Kobe 657-8501, Japan.

Abstract—To develop a specific inhibitor of abscisic acid (ABA) 8'-hydroxylase, a key enzyme in the catabolism of ABA, a plant hormone involved in stress tolerance, seed dormancy, and other various physiological events, we designed and synthesized conformationally restricted analogues of uniconazole (UNI), a well-known plant growth retardant, which inhibits a biosynthetic enzyme (*ent*-kaurene oxidase) of gibberellin as well as ABA 8'-hydroxylase. Although most of these analogues were less effective than UNI in inhibition of ABA 8'-hydroxylase and rice seedling growth, we found that a lactol-bridged analogue with an imidazole is a potent inhibitor of ABA 8'-hydroxylase but not of plant growth. This compound, abscinazole-F1, induced drought tolerance in apple seedlings upon spray treatment with a 10 μM solution.

1. Introduction

Uniconazole-P, *S*-(+)-uniconazole [*S*-(+)-*E*-1-(4-chlorophenyl)-4,4-dimethyl-2-(1,2,4-triazo-1-yl)-1-penten-3-ol, UNI], is an azole-containing cytochrome P450 inhibitor developed as a plant growth retardant in the 1980s.[1,2] UNI has since been used as a plant growth regulator in agriculture and horticulture. The main site of action of UNI is suggested to be *ent*-kaurene oxidase (CYP701A), which catalyzes the three-step oxidation of *ent*-kaurene to *ent*-kaurenoic acid,[3] biosynthetic precursors of the plant hormone gibberellin (GA). This has prompted researchers to use UNI as a chemical tool inhibiting GA biosynthesis. However, UNI also inhibits brassinosteroid biosynthesis[4,5] and alters the level of other plant hormones, such as auxins, cytokinins, ethylene and abscisic acid (ABA).[6] Recently, Kitahata et al.[7] and Saito et al.[8] revealed that UNI strongly inhibits ABA 8'-hydroxylase (CYP707A[9,10]), a key enzyme in ABA catabolism (Figure 1).

Azole-type inhibitors bind to P450 active sites by both coordinating to the heme-iron atom and interacting with surrounding protein residues. Because heme coordination is a common property of azole-containing inhibitors, their affinity and specificity for individual P450 enzymes depend on structural properties other than the azole group. In the case of UNI, these are 4-chlorophenyl and *t*-butyl-hydroxymethyl groups. UNI inhibits various plant P450 enzymes whose native substrates are structurally quite different from each other: e.g., ABA (sesquiterpene) for CYP707A; *ent*-kaurene (diterpene) for CYP701A; and steroids for brassinosteroid biosynthetic enzymes. Mammalian P450 enzymes metabolizing xenobiotics have a large conformational flexibility to adapt to substrates of different sizes.[11] Because some plant P450 species possess xenobiotic detoxification activity,[12] they may be highly flexible in conformation. On the other hand, ABA 8'-hydroxylase has relatively high substrate specificity.[13] If other UNI-inhibiting P450 enzymes involved in biosynthesis and catabolism of plant hormones also have high substrate specificity, even though this has not yet been

investigated in detail, explanations other than enzyme flexibility may be required to explain the adaptation of UNI. From this standpoint, we have been probing why UNI inhibits various plant P450 enzymes. The first reason must be that UNI is small enough to embed itself into various substrate-binding pockets. If UNI just invades the pocket, even if its geometry does not completely coincide with that of the pocket, the structural plasticity of a P450 active site can allow it to fit into the pocket well enough to make the aza nitrogen interact with the heme iron. Thus, enlargement may be an effective approach to increase enzyme specificity. However, this approach will be reported elsewhere.

In a previous study, we found that the conformer preference of UNI analogues partially contributes to affinity for the active site of ABA 8'-hydroxylase.[14] This is the second possible reason that the low specific inhibition of UNI for plant P450 enzymes may depend on its conformational flexibility. We hypothesized that conformational restriction of UNI may have a drastic influence on its affinity to ABA 8'-hydroxylase or other plant P450 enzymes that have narrow ligand specificity. Restriction of conformation is a strategy that has been widely used in drug design to develop potent and selective enzyme inhibitors.[15] Thus, we tested whether this strategy is applicable for a plant P450 enzyme in developing a specific inhibitor of ABA 8'-hydroxylase.

Because UNI has *t*-butyl and hydroxy groups at the 3-position, the rotation of the C2-C3 bond has a great effect on its molecular shape and electrostatic distribution. C2-N1" bond rotation affects the orientation of the aza-nitrogen, which plays an important role in binding to the P450 heme iron. In a previous study,[14] we uncovered four major conformers **A**-**D** of UNI (Figure 2). If each conformer corresponds to a pocket of various P450 enzymes, a conformationally constrained UNI derivative should be more specific than UNI. We searched and found a known UNI derivative, **1**,[16] that is conformationally restricted (Figure 3). Compound **1** has a structure bridged with a carbonyl group between C5" in the triazole ring and the oxygen of the 3-hydroxy in UNI; therefore, it is expected to be restricted in a similar

4

conformation to the **B**-type form of UNI, which is the crystalline structure in MeOH-H$_2$O, and is theoretically estimated to be the most stable conformer in the aqueous phase (Figure 4).[14] Compound **1**, whose C3 stereochemistry was not shown in the literature, was described as a fungicide and plant growth retardant. However, its conformational structure-activity relationship and enzyme selectivity have never been investigated. Thus, we first synthesized compound **1** and examined its inhibitory effect on ABA 8'-hydroxylase and its activity as a plant growth retardant. The results showed that compound **1** functioned as a plant retardant as effectively as UNI, whereas it did not inhibit ABA 8'-hydroxylase at all, unlike UNI. This suggested that a novel, highly specific P450 inhibitor can be produced by conformational restriction. Restriction in a different manner from **1** might produce a selective inhibitor of ABA 8'-hydroxylase that does not inhibit other UNI-inhibited P450s, and thus never cause plant growth inhibition, in contrast to compound **1**. ABA 8'-hydroxylase is a key enzyme in the catabolism of ABA, a plant hormone involved in stress tolerance, seed dormancy, and other physiological events.[17] Thus, a specific inhibitor of ABA 8'-hydroxylase is promising not only as a chemical probe for the mechanism of ABA action, but also because of its potential use in agriculture and horticulture. We synthesized and tested various conformationally restricted analogues (Figure 3) to identify novel inhibitors of ABA 8'-hydroxylase with no growth-retardant effect.

2. Results and Discussion

2.1. Preparation of compound 1 and its properties

Both racemic and optically pure compound **1** were synthesized respectively from racemic and optically pure UNI according to a reported method[16] (Scheme 1). UNI (racemic, *S*, or *R*) was treated with trichloromethyl chloroformate in pyridine to give **1** (racemic, *S*, or *R*). Compound **1** was quite sensitive to light and was partially converted into the *Z*-isomer by

photoisomerization. Although we used a sample stored in the dark as soon as purification was complete, it contained ca. 10% Z-isomer in enzymatic and biological assays. Because the Z-isomer of UNI is much less effective than the corresponding E-isomer in plant growth and ABA 8'-hydroxylase inhibition,[3,7] the activity of **1** will never be overestimated using the Z-isomer-contaminated sample.

The inhibitory activity of **1** against ABA 8'-hydroxylase was examined using recombinant CYP707A3 expressed by *E. coli*. The activity was evaluated based on the decrease in the enzyme product, phaseic acid, caused by addition of a test compound at a concentration two times higher than the substrate S-ABA (5 µM). Inhibitory activity of **1** was much weaker than that of S-UNI (Table 1). The plant growth-retardant effect was examined using rice seedlings. Compound S-**1** exhibited strong activity, although it was weaker than S-UNI (Table 1); the IC_{50} value was 1.3 µM. On the other hand, R-**1** was less effective than the S-isomer; this is the same trend observed for UNI.

The 3D structure of **1**, which was theoretically estimated, is very similar to that of the **B**-type form of UNI (Figure 4). This suggested that conformational freezing of UNI into the **B**-type form results in a decrease in affinity for ABA 8'-hydroxylase with little significant effect on P450 enzymes involved mainly in growth regulation, although the possibility cannot be excluded that the lactone moiety involved in bridging caused the elevated selectivity, independent of conformational freezing. Thus, we designed various UNI analogues (**2-9**) with conformations (**A** and **B**) restricted by different bridge moieties to identify a selective inhibitor of ABA 8'-hydroxylase (Figure 3).

2.2. Design and synthesis of conformationally restricted UNI analogues

2.2.1. B-type restricted analogues. We designed **B**-type restricted analogues with triazole (**2**

and **3**, in addition to **1**) and imidazole rings (**4**, **5** and **6**). A lactone, lactol and cyclic ether were selected for bridging between the azole ring and the oxygen at C3, to compare the effect of these moieties on enzyme selectivity. The triazole types **2** and **3** were prepared from **1** according to Scheme 2. The reduction of **1** with LiAlH$_4$ gave **2** and the ring-opened diol **10**. The reduction of **2** with triethylsilane and trifluoroborane etherate gave the ether-bridged analogue **3**. The imidazole types **4-6** were synthesized from the imidazole analogue of UNI (**11**)[14] according to Scheme 3. Treatment of **11** with trichloromethyl chloroformate gave the lactone-bridged analogue **4**. This compound was reduced with LiAlH$_4$ to give the lactol-bridged analogue **5** and the ring-opened diol **12**. Each stereoisomer of **5** at C3 was prepared from optically pure **11**. However, the stereoisomers derived from the lactol moiety were unable to be resolved because of rapid interconversion. ^{1}H NMR analysis revealed that the diastereomeric ratio was 3:1 in methanol and 5:1 in chloroform, although the absolute configuration of the major diastereomer could not be determined. The intramolecular dehydrated condensation of **12** with ZnCl$_2$ on heating gave mainly **6Z** with *E* to *Z* isomerization. Photoisomerization of **6Z** gave the ether-bridged analogue **6**.

2.2.2. A-type restricted analogues. A similar bridging strategy to that in compound **1** cannot be used for **A**-type restriction of UNI because the aza nitrogen (N2″) of the triazole ring cannot be attached to a bridging moiety without breaking the triazole ring. Thus, we used only the imidazole ring for constructing the **A**-type restricted compound. Our previous report suggests that the replacement of triazole by imidazole has no significant effect on inhibitory activity on ABA 8′-hydroxylase.[14]

The **A**-type restricted analogues **7** and **9** were synthesized from commercially available 5-hydroxymethylimidazole according to Scheme 4. A coupling reaction of the TBS-protected 5-hydroxymethylimidazole **13** and 1-bromo-3,3-dimethylbutan-2-one gave compound **14**. Aldol condensation of **14** and 4-chlorobenzaldehyde gave the ketone **15** as an *E/Z* mixture (1:1), which was UV-irradiated (365 nm) to increase the population of the *E*-isomer by

photoisomerization. The *E*-ketone **15E** was reduced to give **16**, which was deprotected to afford the diol **17**. MnO$_2$ oxidation of **17** gave the lactone-bridged analogue **7** and the aldehyde **18**, whereas ZnCl$_2$ treatment of **17** gave the ether-bridged analogue **9**. This analogue was optically resolved by HPLC using chiral stationary phases. The absolute configuration of optically pure **9** was determined based on Cotton effects in the circular dichroism spectrum (see supplementary data): (+)-**9** is *S*-**9**, and (−)-**9** is *R*-**9**. The aldehyde **18** is the tautomeric isomer (ring-opened form) of the lactol-bridged analogue **8** (ring-closed form), which was not identified in the reaction products. The isolated **18** was stable enough to remain unconverted to the closed form **8** in both protic and aprotic solvents. The opened form **18** seems to be thermodynamically more stable than the closed form **8**. On the other hand, the lactol-bridged analogues **2** and **5** were stable enough to remain unconverted to the ring-opened form. The thermodynamic instability of the lactol-bridged **A**-type analogues contrasts with that of **B**-type analogues, although the reason is not clear.

2.3. Inhibitory potency against ABA 8'-hydroxylase

The inhibitory activity of conformationally restricted analogues **1-7** and **9** against ABA 8'-hydroxylase was examined using Arabidopsis CYP707A3 expressed by *E. coli* (Table 1). First of all, the activity of all the analogues was screened at twice the concentration of the substrate (*S*-ABA). For the **A**-type, the cyclic ether-bridged analogue **9** showed significant inhibition, whereas for the **B**-type, only the lactol-bridged analogues **2** and **5** exhibited more than 50% inhibition; **5** was an especially strong inhibitor, as was **9**. Other analogues of both types were poor inhibitors. The cyclic ether-bridged compounds (**3**, **6**, and **9**), which are the most simple conformationally restricted UNI analogues, have no additional functional group compared to the 3-methoxy-UNI. 3-Methoxy-UNI is as effective as *S*-UNI.[14] This means that the effect of conformational restriction is dominant in the interaction with the active site. Therefore, the difference in CYP707A3 inhibition between the **A**-type (**9**) and **B**-type (**3** and

6) suggests that the CYP707A3 active site prefers the **A**-type conformation of *S*-UNI. On the other hand, for the lactol- and lactone-bridged analogues, this conformational preference was not true, probably because the additional hydroxy and carbonyl groups were advantageous or disadvantageous according to the orientation in the active site. The potent activity of **B**-type analogues **2** and **5** indicates that the lactol moiety of the **B**-type analogue has a significant role in binding to compensate for the conformational disadvantage.

The most potent analogues **5** and **9** were examined in greater detail for each stereoisomer at C3. Kinetic analysis revealed that these analogues function as competitive inhibitors (Figure 5); however, the affinity to the enzyme active site was estimated to be less than one-tenth that of *S*-UNI on the basis of the K_I values. Interestingly, 3*R*-**5** was slightly more effective than the 3*S*-enantiomer (K_I = 420 and 970 nM, respectively), unlike the case of UNI. Analogue **5** may fit into the active site of ABA 8'-hydroxylase in quite a different manner from UNI, because of its **B**-type conformational rigidity and lactol moiety. We cannot discuss this in greater detail due to the lack of structural characterization of ABA 8'-hydroxylase.

2.4. Potency as a plant retardant

UNI, especially the *S*-enantiomer, functions as a highly potent plant retardant, mainly because of its inhibition of *ent*-kaurene oxidase (CYP701A), a biosynthetic enzyme of GA.[3] In fact, *S*-UNI strongly inhibited elongation of rice (cultivar Nipponbare) seedlings even at 300 nM in our assay conditions (Figure 6). In the same bioassay, the inhibitory activity of conformationally restricted analogues of UNI declined by at least a factor of ten compared to *S*-UNI on the basis of the IC$_{50}$ values (Table 1). In an early stage of this study, the potent retardant activity of **1** implied that the **B**-type analogues function as growth inhibitors, whereas the **A**-type analogues never do. However, the **A**-type analogues **7** and **9** were active; in particular, the simplest, ether-bridged **A**-type analogue **9** was more potent than the

corresponding **B**-types **3** and **6**. Moreover, the lactone- and lactol-bridged **B**-type analogues with an imidazole, **4** and **5**, showed no significant inhibition even at 100 μM (Figure 6). Because the corresponding **B**-type analogues with a triazole, **1** and **2**, acted as potent retardants, the 2"-aza nitrogen in the azole ring of the lactone- and lactol-bridged **B**-type analogues may be involved in binding to the active site. These results suggest that the **A**/**B** conformation does not affect primarily the binding to the active site of P450 enzymes involved in rice seedling growth that is represented by CYP701A. Because plant phenotypes can be affected by many factors other than the direct action of an enzyme inhibitor to the target, including uptake, metabolism, and unexpected side effects, we cannot directly discuss the structure-activity relationships for a specific enzyme, e.g. CYP701A, on the basis of findings in this bioassay. Nevertheless, the absence of an effect of **4** and **5** on rice seedling growth indicates that these compounds do not inhibit enzymes involved in growth under our experimental conditions. In future studies, we plan to examine the inhibitory activity of these analogues using recombinant CYP701A and other plant P450 enzymes.

2.5. Drought tolerance induced by abscinazole-F1 (Abz-F1) (5)

In enzymatic and biological assays, all the analogues were less effective than UNI to a greater or lesser extent. This suggests that the rigid conformation confers a basic disadvantage in binding to ABA 8'-hydroxylase and P450 enzymes involved in plant growth, probably because of a decrease in induced fit. However, because the strength of this effect was different for inhibition of ABA 8'-hydroxylase and rice seedling growth, we identified analogue **5**, which we named abscinazole-F1 (Abz-F1), as a new azole-containing inhibitor of ABA 8'-hydroxylase with no inhibition of plant growth. Abz-F1 was too stable to be converted to the Z-isomer and decomposed in the usual conditions in the laboratory.

To determine whether in vivo inhibition of Abz-F1 against ABA 8'-hydroxylase is enough to intensify ABA-induced physiological responses, we tested the effect of Abz-F1 on stomatal aperture and drought tolerance. We tested on 90-day-old apple seedlings by spraying them with an aqueous solution containing the 3R isomer of Abz-F1 at concentrations of 10, 50, and 100 μM. Application of 3R-Abz-F1 before dehydration induced stomatal closure during dehydration (Figure 7) and drought tolerance (Figure 8) as effectively as that of S-UNI at all the tested concentrations. In the 100 μM S-UNI treatment, leaf browning was observed. This side effect, which may have been caused by inhibition of other enzymes including P450s, was also observed to a minor extent following 100 μM 3R-Abz-F1 treatment. Figure 9 shows that 10 μM 3R-Abz-F1 treatment induced slightly stronger drought tolerance in apple seedlings than S-UNI treatment at the same concentration. This is contrary to the finding that the in vitro inhibitory activity of S-UNI for ABA 8'-hydroxylase was much higher than that of 3R-Abz-F1 on the basis of K_I values for the recombinant Arabidopsis enzyme (Table 1). In addition to a difference between the recombinant Arabidopsis and endogenous apple enzymes, this inconsistency may be explained by the phenotypes resulting after treatment with an enzyme inhibitor being affected not only by inhibitory activity against the target enzyme, but also by other factors including uptake, stability, metabolism, and unexpected side effects. The mechanism of action of these azole compounds should be investigated in detail at the enzymatic, cellular, and organ levels. Nevertheless, the present findings at least show that Abz-F1 is an inhibitor of ABA 8'-hydroxylase with no growth-retardant effect, unlike UNI.

3. Conclusions

We focused on conformational flexibility of UNI to identify a specific inhibitor of ABA 8'-hydroxylase, and synthesized conformationally restricted UNI analogues that are bridged between the azole ring and hydroxy group at the C3 position. Most of these analogues showed a decrease in inhibitory activity on ABA 8'-hydroxylase and growth of rice seedlings. This

may be because the decrease in conformational flexibility results in poor binding to the P450 active site. Because the magnitude of this negative effect must differ in different enzymes, the inhibition spectrum of conformationally restricted UNI analogues in plant P450 enzymes should differ from that of UNI. This may be why we found Abz-F1, a new azole-containing inhibitor of ABA 8'-hydroxylase with no inhibition of plant growth. Abz-F1 is the most specific inhibitor against ABA 8'-hydroxylase, although it is not the strongest on the basis of in vitro enzyme assays.

4. Experimental

4.1. General

S-(+)- and R-(−)-uniconazole were prepared by the chiral HPLC purification of uniconazole-P, which was purchased from Wako Pure Chemical Industries, Ltd., Osaka, Japan.[18] (+)-ABA was a gift from Toray Industries Inc., Tokyo, Japan. ^{1}H NMR spectra were recorded with tetramethylsilane as the internal standard using a JEOL JNM-EX270 (270 MHz) and JNM-LA500 (500 MHz) NMR spectrometer. ^{13}C NMR and 2D-correlation NMR experiments were recorded using a JNM-LA500 (500 MHz) NMR spectrometer. High resolution mass spectra were obtained with a JEOL JMS-T100LC "AccuTOF". Optical rotations were recorded with a Jasco DIP-1000 digital polarimeter. Circular dichroism spectra were recorded with a Jasco J-805 spectrophotometer. Column chromatography was performed on silica gel (Wakogel C-200).

4.2. Synthesis of optically pure (E)-1-(4-chlorophenyl)-4,4-dimethyl-2-(1H-1,2,4-triazol-1-yl)pent-1-en-3-ol (1)

S- and R-**1** were synthesized according to the method of Saito et al.[16] To a stirred solution of S-(+)-uniconazole (7 mg, 24.0 μmol) in dry CH_2Cl_2 (0.5 mL) and dry pyridine (50 μL) was added trichloromethyl chloroformate (80 mg, 404 μmol) at 0 °C. The mixture was stirred for 2 h at 0 °C. After being quenched with H_2O at the same temperature, the resulting mixture was extracted with EtOAc (20 mL × 3). The organic layer was washed with H_2O, dried over Na_2SO_4, and concentrated in vacuo. The residual oil was purified by silica gel column chromatography with 20% EtOAc in hexane to obtain S-**1** (7.5 mg, 23.6 μmol, 98%) as colorless oil. R-**1** (5.7 mg, 17.9 μmol) was prepared from R-(−)-uniconazole (6 mg 20.5 μmol)

in 87% yield in the similar manner to the preparation of *S*-**1**. Optical purity of each enantiomer was more than 99% based on HPLC in a chiral column (Daicel Chiralpak AD-H, 250 mm × 4.6 mm, 10% 2-propanol in hexane, 1 mL min^{-1}, 254 nm). Each enantiomer contains the corresponding *Z*-isomer (ca. 15%, determined by ^{1}H NMR) which could not be removed by purification. *S*-**1**: ^{1}H NMR (270 MHz, CD$_3$OD): δ 0.75 (9H, s, *t*-butyl), 5.84 (1H, d, *J* = 0.7 Hz, H-3), 7.51 (4H, m, 4-Cl-phenyl), 7.67 (1H, s, H-1), 8.36 (1H, s, H-3"); UV λ$_{max}$ (MeOH) nm (ε): 297 (10,500) and shoulders at around 224 and 246 nm; HRMS (ESI-TOF, positive mode): calcd for C$_{16}$H$_{16}$ClN$_3$O$_2$Na [M+Na]$^+$ 340.0829, found 340.0827; $[α]_D^{26}$ −18.1 (MeOH, *c* 0.555). *R*-**1**: ^{1}H NMR (270 MHz, CD$_3$OD): δ 0.74 (9H, s, *t*-butyl), 5.84 (1H, d, *J* = 0.7 Hz, H-3), 7.51 (4H, m, 4-Cl-phenyl), 7.67 (1H, s, H-1), 8.37 (1H, s, H-3"); UV λ$_{max}$ (MeOH) nm (ε): 297 (10,300) and shoulders at around 223 and 247 nm; HRMS (ESI-TOF, positive mode): calcd for C$_{16}$H$_{16}$ClN$_3$O$_2$Na [M+Na]$^+$ 340.0829, found 340.0827; $[α]_D^{26}$ +16.3 (MeOH, *c* 0.555). Racemic **1** was prepared in the similar manner to the preparation of optically pure **1**. The spectral data of racemic **1** agreed with that of optically pure **1**.

4.3. Synthesis of 2 and 3

4.3.1. (*E*)-6-*tert*-butyl-5-(4-chlorobenzylidene)-6,8-dihydro-5*H*-[1,2,4]triazolo[5,1-*c*][1,4]oxazin-8-ol (2).

To a stirred solution of **1** (103 mg, 324 μmol) in dry Et$_2$O (20 mL) was added LiAlH$_4$ (29 mg, 763 μmol) at 0 °C. The mixture was stirred for 1 h at the same temperature, then for 1.5 h at room temperature before added LiAlH$_4$ (4 mg). The mixture was stirred for 2 h at room temperature. After quenched with 1 M HCl, the resulting mixture was extracted with EtOAc (80 mL × 3). The organic layer was washed with H$_2$O, dried over Na$_2$SO$_4$, and concentrated in vacuo. The residual oil was purified by column chromatography on silica gel with 30% EtOAc in hexane to give **2** (48 mg, 151 μmol, 47%) as a diastereomeric mixture (59:41, determined by integrating H-3 singlets in the ^{1}H NMR spectrum) and **10** (21 mg, 65 μmol, 20%) as colorless oils. **2**: ^{1}H NMR (270 MHz, CDCl$_3$):

major diastereomer: δ 0.70 (9H, s, *t*-butyl), 5.17 (1H, s, H-3), 6.51 (1H, s, -(HO)**H**C-5"), 7.36 (m, 4-Cl-phenyl, overlapped with H-1), 7.41 (s, H-1, overlapped with 4-Cl-phenyl protons), 8.03 (1H, s, H-3"); minor diastereomer: δ 0.74 (9H, s, *t*-butyl), 5.12 (1H, s, H-3), 6.43 (1H, s, -(HO)**H**C-5"), 7.36 (m, 4-Cl-phenyl, overlapped with H-1), 7.37 (s, H-1, overlapped with 4-Cl-phenyl protons), 8.05 (1H, s, H-3"); UV λmax (MeOH) nm (ε): 270 (17,800); HRMS (ESI-TOF, positive mode): calcd for $C_{16}H_{18}ClN_3O_2Na$ [M+Na]$^+$ 342.0985, found 342.0982.

10: ^{1}H NMR (270 MHz, CDCl$_3$): δ 0.66 (9H, s, *t*-butyl), 4.50 (1H, d, *J* = 8.9 Hz, H-3), 4.78 (1H, d, *J* = 8.9 Hz, HO-3), 4.83 (1H, d, *J* = 13.8 Hz, -H$_2$C-5"), 4.98 (1H, d, *J* = 13.8 Hz, -H$_2$C-5"), 6.98 (1H, s, H-1), 7.39 (4H, m, 4-Cl-phenyl), 7.97 (1H, s, H-3"); UV λmax (MeOH) nm (ε): 250 (13,400); HRMS (ESI-TOF, positive mode): calcd for $C_{16}H_{20}ClN_3O_2Na$ [M+Na]$^+$ 344.1142, found 344.1143.

4.3.2. (*E*)-6-*tert*-butyl-5-(4-chlorobenzylidene)-6,8-dihydro-5*H*-[1,2,4]triazolo[5,1-*c*][1,4]oxazine (3). To a stirred solution of **2** (30 mg, 93 μmol) in dry CH$_2$Cl$_2$ (2 mL) was added triethylsilane (100 μL) and boron trifluoride diethyl etherate (100 μL) at room temperature. The mixture was stirred for 12 d at room temperature. After quenched with sat. NaHCO$_3$, the resulting mixture was extracted with EtOAc (20 mL × 3). The organic layer was washed with H$_2$O, dried over Na$_2$SO$_4$, and concentrated in vacuo. The residual oil was purified by column chromatography on silica gel with 10% EtOAc in hexane and then further purified by reverse-phase HPLC (YMC-Pack ODS-AQ, 150 × 20 mm, 80% MeOH, 4 mL min^{-1}, 254 nm) to give **3** (3.7 mg, 12 μmol, 13%) as colorless crystalline solid and its *Z*-isomer (1.3 mg). **3**: ^{1}H NMR (270 MHz, CDCl$_3$): δ 0.75 (9H, s, *t*-butyl), 4.94 (1H, s, H-3), 5.06 (1H, d, *J* = 16.8 Hz, -H$_2$C-5"), 5.18 (1H, d, *J* = 16.8 Hz, -H$_2$C-5"), 7.33 (4H, m, 4-Cl-phenyl), 7.42 (1H, s, H-1), 8.00 (1H, s, H-3"); UV λmax (MeOH) nm (ε): 269 (11,800), 213 (6,400); HRMS (ESI-TOF, positive mode): calcd for $C_{16}H_{19}ClN_3O$ [M+H]$^+$ 304.1217, found 304.1213. *Z*-isomer of **3**: ^{1}H NMR (270 MHz, CDCl$_3$): δ 0.92 (9H, s, *t*-butyl), 4.22 (1H, s, H-3), 4.98 (1H, d, *J* = 16.2 Hz, -H$_2$C-5"), 5.15 (1H, d, *J* = 16.2 Hz, -H$_2$C-5"), 6.19 (1H, s, H-1), 7.33 (4H, m, 4-Cl-phenyl), 7.91 (1H, s, H-3"); UV λmax (MeOH) nm (ε): 274 (8,600),

219 (7,200); HRMS (ESI-TOF, positive mode): calcd for $C_{16}H_{19}ClN_3O$ [M+H]$^+$ 304.1217, found 304.1214.

4.4. Synthesis of 4, 5, and 6

4.4.1. (*E*)-6-*tert*-butyl-5-(4-chlorobenzylidene)-5*H*-imidazo[2,1-*c*][1,4]oxazin-8(6*H*)-one

(**4**). To a stirred solution of compound **11**[14] (0.556 g, 1.9 mmol) in dry MeCN (250 mL) under Ar was added pyridine (1.47 g, 19 mmol) and trichloromethyl chloroformate (1.28 g, 7.15 mmol) at 0 °C. The mixture was stirred for 4 h at the same temperature. After quenched with H_2O, MeCN was removed from the mixture in vacuo before extracted with EtOAc (70 mL × 3). The organic layer was washed with brine, dried over Na_2SO_4, and concentrated in vacuo. The residual oil was purified by column chromatography on silica gel with 30% EtOAc in hexane to give **4** (0.567 g, 1.79 mmol, 94%) as pale yellow oil. **4**: ^{1}H NMR (500 MHz, CD_3OD): δ 0.73 (9H, s, *t*-butyl), 5.58 (1H, s, H-3), 7.33 (1H, s, H-1), 7.43 (1H, s, triazole), 7.47 (4H, m, 4-Cl-phenyl), 7.98 (1H, s, triazole); UV λmax (MeOH) nm (ε): 259 (13,300); HRMS (ESI-TOF, positive mode): calcd for $C_{17}H_{17}ClN_2O_2Na$ [M+Na]$^+$ 339.0876, found 339.0874.

4.4.2. (*E*)-6-*tert*-butyl-5-(4-chlorobenzylidene)-6,8-dihydro-5*H*-imidazo[2,1-*c*][1,4]oxazin-8-ol (5). To a stirred solution of **4** (31.6 mg, 0.100 mmol) in dry Et_2O (0.5 mL) was added $LiAlH_4$ (16 mg, 0.34 mmol) at 0 °C. The mixture was stirred for 1 h at the same temperature. After quenched with 1 M HCl, the resulting mixture was extracted with EtOAc (20 mL × 4). The organic layer was washed with brine, dried over Na_2SO_4, and concentrated in vacuo. The residual oil was purified by column chromatography on silica gel with 30% acetone in hexane to give **5** (12.3 mg, 0.038 mmol, 38%) which was a diastereomeric mixture (3:1 in $CDCl_3$, and 5:1 in CD_3OD, determined by ^{1}H NMR) as pale yellow powder and the lactone ring-opened diol **12** (7.6 mg, 0.023 mmol, 24%) as pale yellow powder. **5**: ^{1}H NMR (500

MHz, CD$_3$OD): major diastereomer: δ 0.63 (9H, s, *t*-butyl), 5.06 (1H, s, H-3), 6.16 (1H, s, -(HO)**H**C-2"), 6.93 (1H, s, H-1), 7.08 (1H, s, triazole), 7.38 (4H, s, 4-Cl-phenyl), 7.41 (1H, s, triazole); minor diastereomer: δ 0.71 (9H, s, *t*-butyl), 4.94 (1H, s, H-3), 6.07 (1H, s, -(HO)**H**C-2"), 6.98 (1H, s, H-1), 7.12 (1H, s, triazole), 7.38 (4H, s, 4-Cl-phenyl), 7.60 (1H, s, triazole); UV λmax (MeOH) nm (ε): 264 (17,300); HRMS (ESI-TOF, positive mode): calcd for C$_{17}$H$_{20}$ClN$_2$O$_2$ [M+H]$^+$ 319.1213, found 319.1210. **12**: ^{1}H NMR (500 MHz, CD$_3$OD): δ 0.69 (9H, s, *t*-butyl), 4.52 (1H, s, H-3), 4.70 (1H, d, *J* = 12.8 Hz, (HO)**H**$_2$C-2"), 4.76 (1H, d, *J* = 12.8 Hz, (HO)**H**$_2$C-2"), 6.79 (2H, s, H-1 and triazole), 7.43 (4H, m, 4-Cl-phenyl), 7.57 (1H, s, triazole); UV λmax (MeOH) nm (ε): 250 (13,800); HRMS (ESI-TOF, positive mode): calcd for C$_{17}$H$_{22}$ClN$_2$O$_2$ [M+H]$^+$ 321.1370, found 321.1367. The 3*S* and 3*R* epimers of **5** were prepared from optically pure **17**[12] by the similar manner for the preparation of the epimeric mixture **5**. 3*S*-**5**: ^{1}H NMR (270 MHz, acetone-*d*$_6$): δ 0.63 (9H, s, *t*-butyl), 5.08 (1H, s, H-3), 6.17 (1H, s, -(HO)**H**C-2"), 6.92 (1H, s, H-1), 7.01 (1H, d, *J* = 1.3 Hz, triazole), 7.46 (4H, s, 4-Cl-phenyl), 7.48 (1H, d, *J* = 1.3 Hz, triazole); HRMS (ESI-TOF, positive mode): calcd for C$_{17}$H$_{19}$ClN$_2$O$_2$Na [M+Na]$^+$ 341.1033, found 341.1030. 3*R*-**5**: ^{1}H NMR (270 MHz, acetone-*d*$_6$): δ 0.63 (9H, s, *t*-butyl), 5.08 (1H, s, H-3), 6.17 (1H, s, -(HO)**H**C-2"), 6.92 (1H, s, H-1), 7.01 (1H, d, *J* = 1.3 Hz, triazole), 7.46 (4H, s, 4-Cl-phenyl), 7.49 (1H, d, *J* = 1.3 Hz, triazole); HRMS (ESI-TOF, positive mode): calcd for C$_{17}$H$_{19}$ClN$_2$O$_2$Na [M+Na]$^+$ 341.1033, found 341.1029.

4.4.3. (Z)-6-*tert*-butyl-5-(4-chlorobenzylidene)-6,8-dihydro-5*H*-imidazo[2,1-*c*][1,4]oxazine (6Z). To a stirred solution of **12** (18.5 mg, 58 μmol) in dry 1,2-dichloroethane (1 mL) was added ZnCl$_2$ (70 mg, 510 μmol) at room temperature. The mixture was stirred for 6 h at 100 °C. After quenched with H$_2$O, the resulting mixture was extracted with CH$_2$Cl$_2$ (25 mL × 3). The organic layer was washed with brine, dried over Na$_2$SO$_4$, and concentrated in vacuo. The residual oil was purified by column chromatography on silica gel with 30% acetone in hexane to give **6Z** (9.0 mg, 29 μmol, 51%) as pale red oil. **6Z**: ^{1}H NMR (270 MHz, CDCl$_3$): δ 0.89 (9H, s, *t*-butyl), 4.17 (1H, s, H-3), 4.80 (1H, d, *J* = 14.5 Hz, -O-H$_2$C-2"), 5.00 (1H, d, *J* =

14.5 Hz, -O-H$_2$C-2"), 6.11 (1H, s, H-1), 6.61 (1H, s, triazole), 6.93 (1H, s, triazole), 7.12 and 7.28 (each 2H, m, 4-Cl-phenyl).

4.4.4. (*E*)-6-*tert*-butyl-5-(4-chlorobenzylidene)-6,8-dihydro-5*H*-imidazo[2,1-*c*][1,4]oxazine (6).

A solution of **6Z** (9.0 mg, 29 μmol) in EtOAc (2 mL) was irradiated with UV light (365 nm, UVP B-100A) for 12 h. After concentrated in vacuo, the residual oil was purified by column chromatography on silica gel with 30% EtOAc in hexane to give **6** (2.9 mg, 29 μmol, 32%) as pale yellow oil. **6**: ^{1}H NMR (500 MHz, acetone-d_6): δ 0.72 (9H, s, *t*-butyl), 4.84 (1H, d, *J* = 15.6 Hz, -O-H$_2$C-2"), 4.91 (1H, s, H-3), 5.02 (1H, d, *J* = 15.6 Hz, -O-H$_2$C-2"), 7.01 (1H, s, H-1), 7.04 (1H, d, *J* = 1.2 Hz, triazole), 7.44 (4H, m, 4-Cl-phenyl), 7.63 (1H, d, *J* = 1.2 Hz, triazole); ^{13}C NMR (125 MHz, acetone-d_6): δ 27.2 (methyls in *t*-butyl), 38.8 (tertiary carbon of *t*-butyl), 61.9 (C6'), 77.0 (C3), 114.5 (C4" or C5"), 116.2 (C1), 129.6 (4-Cl-phenyl), 130.3 (C4" or C5"), 131.6 (4-Cl-phenyl), 133.4 and 133.5 (C1' and C2), 143.1 (C2"); UV λmax (MeOH) nm (ε): 264 (14,300); HRMS (ESI-TOF, positive mode): calcd for C$_{17}$H$_{20}$ClN$_2$O [M+H]$^+$ 303.1264, found 303.1267.

4.5. Synthesis of 7 and 9

4.5.1. 5-((*tert*-butyldimethylsilyloxy)methyl)-1*H*-imidazole (13).

TBS-protected 5-hydroxymethylimidazole (**13**) (5.9 g, 27.8 mmol) was prepared from commercially available 4(5)-hydroxymethylimidazole hydrochloride (5.0 g, 37.2 mmol) in 75% yield according to the method of Amino et al.[19] ^{1}H NMR spectrum of **13** was coincident with that reported by Amino et al.[16]

4.5.2. 1-(5-((*tert*-butyldimethylsilyloxy)methyl)-1*H*-imidazol-1-yl)-3,3-dimethylbutan-2-one (14).

To a stirred solution of **13** (5.88 g, 27.9 mmol) in dry Et$_2$O (110 mL) was added sodium hydride (60% in oil, 0.75 g, 31.2 mmol) at 0 °C. The mixture was stirred for 0.5 h at

the same temperature before being added dropwise 1-bromo-3,3-dimethyl-2-butanone (5.45 g, 30.5 mmol). The mixture was stirred for 1 h at 0 °C. After quenched with H_2O, the resulting mixture was extracted with EtOAc (100 mL × 3). The organic layer was washed with H_2O, dried over Na_2SO_4, and concentrated in vacuo. The residual oil was purified by silica gel column chromatography with 20–40% acetone in hexane to obtain **14** (0.76 g, 2.45 mmol, 9%) and its 4-substituted isomer (2.17 g, 6.99 mmol, 25%) as pale yellow oil. **14**: ^{1}H NMR (500 MHz, CDCl$_3$): δ 0.01 (6H, s, two methyls of TBS), 0.85 (9H, s, *t*-butyl of TBS), 1.26 (9H, s, *t*-butyl), 4.51 (2H, s, -H$_2$C-5'), 5.04 (2H, s, H$_2$-1), 6.89 (1H, s, H-4'), 7.34 (1H, s, H-2'); ^{13}C NMR (125 MHz, CDCl$_3$): −5.36 (C2''), 18.1 (C3''), 25.8 and 26.3 (C4 and C4''), 43.3 (C3), 49.3 (C1), 55.5 (C1''), 127.7 (C4'), 130.7 (C5'), 139.3 (C2'), 207.8 (C2); HRMS (ESI-TOF, positive mode): calcd for C$_{16}$H$_{30}$N$_2$O$_2$SiNa [M+Na]$^+$ 333.1974, found 333.1971. The substituted position in the imidazole ring of **14** was determined based on an HMBC correlation: -C(O)-C**H**$_2$-N-**C**(CH$_2$OTBS)=CH-.

4.5.3. (*Z* and *E*)-2-(5-((*tert*-butyldimethylsilyloxy)methyl)-1*H*-imidazol-1-yl)-1-(4-chlorophenyl)-4,4-dimethylpent-1-en-3-one (15Z and 15E).

To a stirred solution of **14** (2.2 g, 7.1 mmol) in Ac$_2$O (25 mL) was added K$_2$CO$_3$ (1.3 g, 9.7 mmol) and *p*-chlorobenzaldehyde (1.2 g, 8.5 mmol) at the room temperature. The mixture was stirred for 3 h at 100 °C. After quenched with sat. NaHCO$_3$, the resulting mixture was extracted with EtOAc (150 mL × 3). The organic layer was washed with H$_2$O, dried over Na$_2$SO$_4$, and concentrated in vacuo. The residual oil was purified by silica gel column chromatography with 20% EtOAc in hexane to obtain a mixture (1:1, based on TLC) of **15Z** and **15E** (1.9 g, 4.4 mmol, 62%) as pale yellow oil.

4.5.4. (*E*)-2-(5-((*tert*-butyldimethylsilyloxy)methyl)-1*H*-imidazol-1-yl)-1-(4-chlorophenyl)-4,4-dimethylpent-1-en-3-one (15E).

The solution of a mixture of **15Z** and **15E** (1.9 g, 4.4 mmol) in EtOAc (100 mL) was irradiated with UV light (365 nm, UVP B-100A) for 14 h. After concentrated in vacuo, the residual oil was purified by column

chromatography on silica gel with 20% EtOAc in hexane to give **15E** (1.2 g, 2.8 mmol, 63%) as pale yellow oil. **15E**: ^{1}H NMR (270 MHz, acetone-d_6): δ 0.13 (6H, s, two methyls of TBS), 0.90 (9H, s, t-butyl of TBS), 0.97 (9H, s, t-butyl), 4.80 (2H, s, -H$_2$C-5'), 7.08 (1H, s, H-4"), 7.22 (1H s, H-1), 7.43 (2H, m, 4-Cl-phenyl), 7.47 (2H, m, 4-Cl-phenyl), 7.65 (1H, d, J = 1.3 Hz, H-2"); HRMS (ESI-TOF, positive mode): calcd for C$_{23}$H$_{33}$ClN$_2$O$_2$SiNa [M+Na]$^+$ 455.1898, found 455.1896.

4.5.5. (*E*)-2-(5-((*tert*-butyldimethylsilyloxy)methyl)-1*H*-imidazol-1-yl)-1-(4-chlorophenyl)-4,4-dimethylpent-1-en-3-ol (16).

To a stirred solution of **15E** (1.2 g, 2.8 mmol) in MeOH (45 mL) was added NaBH$_4$ (220 mg, 5.8 mmol) at 0 °C. The mixture was stirred for 1 h at room temperature. After quenched with sat. NH$_4$Cl, the resulting mixture was extracted with EtOAc (50 mL × 3). The organic layer was washed with H$_2$O, dried over Na$_2$SO$_4$, and concentrated in vacuo. The residual oil was purified by column chromatography on silica gel with 20% acetone in hexane to give **16** (0.6 g, 1.4 mmol, 49%) as white solid. **16**: ^{1}H NMR (270MHz, CDCl$_3$): δ 0.14 (3H, s, methyl of TBS), 0.17 (3H, s, methyl of TBS), 0.73 (9H, s, t-butyl of TBS), 0.93 (9H, s, t-butyl), 4.39 (1H, d, J = 8.5 Hz, H-3), 4.53 (1H, d, J = 8.5 Hz, HO-3), 4.68 (1H, d, J = 13.2 Hz, -H$_2$C-5"), 4.81 (1H, d, J = 13.2 Hz, -H$_2$C-5"), 6.74 (1H, s, H-1), 7.04 (1H, d, J = 1.0 Hz, H-4"), 7.38 (4H, s, 4-Cl-phenyl), 7.70 (1H, s, H-2"); HRMS (ESI-TOF, positive mode): calcd for C$_{23}$H$_{36}$ClN$_2$O$_2$Si [M+H]$^+$ 435.2235, found 435.2234.

4.5.6. (*E*)-1-(4-chlorophenyl)-2-(5-(hydroxymethyl)-1*H*-imidazol-1-yl)-4,4-dimethylpent-1-en-3-ol (17).

To a stirred solution of **16** (0.6 g, 1.4 mmol) in EtOH (60 mL) and H$_2$O (20 mL) was added 1M HCl (10 mL) at room temperature. The mixture was stirred for 1.5 h at room temperature. After quenched with sat. NaHCO$_3$, the resulting mixture was extracted with EtOAc (150 mL × 3). The organic layer was washed with H$_2$O, dried over Na$_2$SO$_4$, and concentrated in vacuo. The residual oil was purified by column chromatography on silica gel with 20% acetone in hexane to give **17** (0.39 g, 1.2 mmol, 89%) as white solid.

17: ^{1}H NMR (270MHz, CDCl$_3$): δ 0.75 (9H, s, *t*-butyl), 4.48 (1H, s, H-3), 4.58 (1H, d, *J* = 13.2 Hz, -H$_2$C-5"), 4.74 (1H, d, *J* = 13.2 Hz, -H$_2$C-5"), 6.68 (1H, s, H-1), 7.00 (1H, s, H-4"), 7.38 (4H, m, 4-Cl-phenyl), 7.72 (1H, s, H-2"); HRMS (ESI-TOF, positive mode): calcd for C$_{17}$H$_{22}$ClN$_2$O$_2$ [M+H]$^+$ 321.1370, found 321.1342.

4.5.7. **(*E*)-6-*tert*-butyl-5-(4-chlorobenzylidene)-5*H*-imidazo[5,1-*c*][1,4]oxazin-8(6*H*)-one (7).** To a stirred solution of **17** (53 mg, 0.17 mmol) in acetone (30 mL) was added MnO$_2$ (activated, 186 mg, 2.14 mmol) at room temperature. The mixture was stirred for 5 h at the same temperature. After filtered MnO$_2$ through a filter paper, the filtrate was concentrated in vacuo. The residual oil was purified by column chromatography on silica gel with 15% acetone in hexane to give **7** (19 mg, 59 μmol, 35%) and **18** (31 mg, 97 μmol, 59%) as white solids. **7**: ^{1}H NMR (270 MHz,CDCl$_3$): δ 0.76 (9H, s, *t*-butyl), 5.32 (1H, s, H-3), 7.05 (1H, s, H-1), 7.36 (4H, m, 4-Cl-phenyl), 7.91 (1H, s, H-4"), 8.08 (1H, s, H-2"); UV λmax (MeOH) nm (ε): 257.0 (14,100); HRMS (ESI-TOF, positive mode): calcd for C$_{17}$H$_{18}$ClN$_2$O$_2$ [M+H]$^+$ 317.1057, found 317.1064. **18**: ^{1}H NMR (270 MHz,CDCl$_3$): δ 0.75 (9H, s, *t*-butyl), 3.95 (1H, s, HO-3), 4.76 (1H, d, *J* = 3.0 Hz, H-3), 6.72 (1H, s, H-1), 7.40 (4H, m, 4-Cl-phenyl), 7.92 (1H, s, H-4"), 7.98 (1H, s, H-2"), 9.74 (1H, s, OHC-5"); UV λmax (MeOH) nm (ε): 257 (15,300); HRMS (ESI-TOF, positive mode): calcd for C$_{17}$H$_{20}$ClN$_2$O$_2$ [M+H]$^+$ 319.1213, found 319.1204.

4.5.8. (*E*)-6-*tert*-butyl-5-(4-chlorobenzylidene)-6,8-dihydro-5*H*-imidazo[5,1-*c*][1,4]oxazine (9). To a stirred solution of **17** (51 mg, 0.16 mmol) in dry dichloroethane (20 mL) was added ZnCl$_2$ (60 mg, 0.44 mmol) at room temperature. The mixture was stirred for 31 h at the same temperature before added H$_2$O. The mixture was extracted with CH$_2$Cl$_2$ (50 mL × 3). The organic layer was washed with brine, dried over Na$_2$SO$_4$, and concentrated in vacuo. The residual oil was purified by column chromatography on silica gel with 20% acetone in hexane to give **9** (13 mg, 43 μmol, 27%) as white solid. **9**: ^{1}H NMR (500 MHz, CDCl$_3$): δ 0.67 (9H, s, *t*-butyl), 4.81 (1H, d, *J* = 14.0 Hz, -H$_2$C-5"), 4.82

(1H, s, H-3), 4.99 (1H, d, J = 14.0 Hz, -H$_2$C-5″), 6.81 (1H, s, H-1), 6.91 (1H, s, H-4″), 7.32 (4H, m, 4-Cl-phenyl), 7.88 (1H, s, H-2″); ^{13}C NMR (125 MHz, CDCl$_3$): δ 26.4 (methyls of t-butyl), 38.2 (tertiary carbon of t-butyl), 59.2 (-H$_2$C-5″), 77.5 (C3), 119.2 (C3), 123.1 (C4″), 127.4 (C5″), 129.0 (C3′ and C5′), 130.2 (C2′ and C6′), 131.4 (C2″), 132.3 (C2), 133.0 (C4′), 133.6 (C1′); UV λmax (MeOH) nm (ε): 265 (15,600); HRMS (ESI-TOF, positive mode): calcd for C$_{17}$H$_{20}$ClN$_2$O [M+H]$^+$ 303.1264, found 303.1264.

4.5.9. Optical resolution of 9. Compound **9** (33 mg) was subjected to chiral HPLC under the following conditions: column, Chiralpak OD-H (250 × 10 mm, Daicel); solvent, 13% 2-propanol in hexane; flow rate, 5 mL min^{-1}; detection, 254 nm. The materials at t_R 14.7 and 30.7 min were collected to give (−)-**9** (14.4 mg) and (+)-**9** (14.0 mg), respectively, with an optical purity of each 99.9%. (+)-**9**: $[\alpha]_D^{24}$ +15.2 (MeOH, c 0.787); CD λmax (MeOH) nm ($\Delta\varepsilon$): 275 (+7.2), 241 (0), 216 (−19.4); ^{1}H NMR (500 MHz, CDCl$_3$): δ 0.67 (9H, s, t-butyl), 4.81 (1H, d, J = 14.0 Hz, -H$_2$C-5″), 4.82 (1H, s, H-3), 4.99 (1H, d, J = 14.0 Hz, -H$_2$C-5″), 6.81 (1H, s, H-1), 6.91 (1H, s, H-4″), 7.32 (4H, m, 4-Cl-phenyl), 7.88 (1H, s, H-2″); HRMS (ESI-TOF, positive mode): calcd for C$_{17}$H$_{20}$ClN$_2$O [M+H]$^+$ 303.1264, found 303.1264. (−)-**9**: $[\alpha]_D^{24}$ −16.2 (MeOH, c 0.600); CD λmax (MeOH) nm ($\Delta\varepsilon$): 275 (−7.1), 244 (0), 214 (+21.0); ^{1}H NMR (500 MHz, CDCl$_3$): δ 0.67 (9H, s, t-butyl), 4.81 (1H, d, J = 14.0 Hz, -H$_2$C-5″), 4.82 (1H, s, H-3), 4.99 (1H, d, J = 14.0 Hz, -H$_2$C-5″), 6.81 (1H, s, H-1), 6.91 (1H, s, H-4″), 7.32 (4H, m, 4-Cl-phenyl), 7.88 (1H, s, H-2″); HRMS (ESI-TOF, positive mode): calcd for C$_{17}$H$_{20}$ClN$_2$O [M+H]$^+$ 303.1264, found 303.1264. See supplementary data for determination of the absolute configuration of optically pure **9**.

4.6. Coexpression of recombinant CYP707A3 and Arabidopsis P450 reductase (AR2) in *Escherichia coli*

A truncated Arabidopsis CYP707A3 (707A3d28), which lacked the putative

membrane-spanning segment of the N-terminus, residues 3-28, was constructed. Cells of *E. coli* strain BL21 were transformed with the pCW-CYP707A3d28 and pACYC-AR2 constructs. Cultures (3 mL) were grown overnight in Luria-Bertani medium supplemented with ampicillin (50 µg mL^{-1}) and chloramphenicol (100 µg mL^{-1}). Then, 50 mL of Terrific Broth medium supplemented with ampicillin (50 µg mL^{-1}), chloramphenicol (100 µg mL^{-1}), and aminolevulic acid (0.5 mM) was inoculated with an aliquot of the overnight culture (0.5 mL). The culture was incubated with gentle shaking (225 rpm) at 37 °C until A$_{600}$ reached 0.6 (for 2.5–3 h), and the expression of the P450 enzyme was induced by the addition of isopropyl-β-D-thiogalactopyranoside (0.1 mM). The culture was shaken continuously (150 rpm) at 25 °C and cells were harvested 48 h later by centrifugation at 2,330 *g* for 20 min at 4 °C. Pelleted cells were suspended in 2.5 mL of Buffer A (50 mM potassium phosphate buffer, pH 7.25, 20% glycerol, 1 mM EDTA, 0.1 mM dithiothreitol). The suspension was sonicated for 30 s, and the enzyme solution in the supernatant was collected by centrifugation at 23,470 *g* for 30 min at 4 °C. The P450 content was determined by spectrophotometric analysis, using the extinction coefficient of reduced CO difference spectrum (91.1 mM^{-1} cm^{-1}).[20]

4.7. Enzyme assay

Kinetic analysis was performed according to the detailed protocols described previously.[13] A reaction mixture containing 25 µg mL^{-1} CYP707A3 microsomes coexpressed AR2 in *E. coli*, (+)-ABA (final conc.: 0.5–128 µM), inhibitors (0 for control, 2-1000 nM, in 5 µL DMF) and 50 µM NADPH in 50 mM potassium phosphate buffer (pH 7.25) were incubated for 10 min at 30 °C. Reactions were initiated by adding NADPH, and stopped by addition of 50 µL of 1 M NaOH. The reaction mixtures were acidified with 100 µL of 1 M HCl. To extract the reaction products, the mixtures were loaded onto Oasis HLB cartridges (1 mL, 30 mg; Waters) and washed with 1 mL of 10% MeOH in H$_2$O containing 0.5% AcOH. The enzyme

products were then eluted with 1 mL of MeOH containing 0.5% AcOH, and the eluate was concentrated in vacuo. The dried sample was dissolved in 50 μL of MeOH, and 10 μL were subjected to HPLC. HPLC conditions were: ODS column, Hydrosphere C18 (150×6.0 mm, YMC); solvent, 35% MeOH or 20% MeCN in H_2O containing 0.1% AcOH; flow rate, 1.0 mL min^{-1}; detection, 254 nm. Enzyme activity was confirmed by determining the amounts of phaseic acid (PA) in control experiments before each set of measurements. Inhibition constants were determined using the Enzyme Kinetics module of SigmaPlot 10 software[21] after determining the mode of inhibition by plotting the reaction velocities in the presence and absence of inhibitor on a double-reciprocal plot. For the non-inhibited enzymatic reaction, the K_M for (+)-ABA was calculated to be 3.4 ± 0.6 μM, based on five separate experiments. All tests were conducted at least three times.

4.8. Bioassays

4.8.1. Rice seedling elongation assay. Seeds of rice (*Oryza sativa* L. cv. Nipponbare) were sterilized with EtOH for 5 min and washed with running tap water. The sterilized seeds were soaked in water to germinate for 3 days at 25 °C. The seeds were then placed in a glass tube (40 mm i.d.) containing 2 mL of a test solution and grown with the tube sealed with a plastic cap under continuous light (10000 lux) at 25 °C. When the seedlings were 7 days old, the length of the second leaf sheath was measured, and the inhibition ratio was calculated. The inhibition ratio is defined as $[(A - B)/A] \times 100$, where A = the mean length of the second leaf sheath when water was used, and B = the mean length of the second leaf sheath when a test compound was used. All tests were conducted at least twice.

4.8.2. Drought tolerance assay. Apple [*Malus sylvestris* (L.) Mill. var. *domestica* (Borkh.) Mansf.] cultivar Akitabeniakari seeds were soaked overnight in water, then sown in moist vermiculite and grown in a greenhouse. Seedlings (90 days old) were divided into two groups:

water-stressed and well-watered. The seedlings of the water-stressed group were sprayed uniformly with 2 mL of a test solution (10, 50, or 100 μM) containing 3*R*-Abz-F1, UNI (positive control), or distilled water (untreated control) before water-stressing them for 150 h, then watering them once, and then water-stressing them again for an additional 330 h. The well-watered group was watered once daily so that the vermiculite was saturated. Measurement of stomatal aperture was performed as follows: the state of 10 stomatal apertures per leaf was observed using a TM-1000 microscope (Hitachi High-Technologies Co., Tokyo, Japan); three leaves from three randomly selected seedlings (one leaf per seedling) were used; that is, 30 stomatal apertures per treatment were measured. The water potential of the vermiculite was measured with a WP4-T water potential meter (Decagon Devices, Inc., USA). Apple [*Malus sylvestris* (L.) Mill. var. *domestica* (Borkh.) Mansf.] cultivar Fuji seeds were soaked overnight in water, then sown in moist vermiculite and grown in a greenhouse. The seedlings were 60 days old at the time of the treatment. Each plant was sprayed uniformly with 2 mL of the test solution. The untreated control group was sprayed with distilled water, and the treated group was sprayed with a solution of 3*R*-Abz-F1 (10 μM) or *S*-UNI (10 μM). All test groups were watered before treatment. The seedlings were water-stressed for 480 h.

4.9. Computational method.

The minimum-energy conformer of compound **1** was generated and minimized using MM3 combined with the molecular dynamics simulation built into CAChe 3.11.[22] This MM3-minimized structure was fully optimized with density functional theory, using the Becke three parameter hybrid functional (B3LYP) method and the 6-31G(d) basis set in Gaussian 03.[23]

Acknowledgments

Supplementary data

Determination of the absolute configuration of optically pure **9**, determination of the *E*- and *Z*-isomers of UNI analogues, and ^{1}H NMR spectra of new compounds which were used in the enzymatical and biological assays, and supplementary data associated with this article can be found in the online version at doi:xx.xxxx/j.bmc.200x.xx.xxx.

References and notes

1. Funaki, Y.; Ishiguri, T.; Kato, T.; Tanaka, S. *J. Pesticide Sci.* **1984**, *9*, 229.

2. Funaki, Y.; Oshita, H.; Yamamoto, S.; Tanaka, S.; Kato, T. (Sumitomo Chemical Co.). Ger. Offen. DE3010560, 1980.

3. Izumi, K.; Kamiya, Y.; Sakurai, A.; Oshio, H.; Takahashi, N. *Plant Cell Physiol.* **1985**, *26*, 821.

4. Iwasaki, T.; Shibaoka, H. *Plant Cell Physiol.* **1991**, *32*, 1007.

5. Asami, T.; Mizutani, M.; Fujioka, S.; Goda, H.; Min, Y. K.; Shimada, Y.; Nakano, T.; Takatsuto, S.; Matsuyama, T.; Nagata, N.; Sakata, K.; Yoshida, S. *J. Biol. Chem.* **2001**, *276*, 25687.

6. Izumi, K.; Nakagawa, S.; Kobayashi, M.; Oshio, H.; Sakurai, A.; Takahashi, N. *Plant Cell Physiol.* **1988**, *29*, 97.

7.   Kitahata, N.; Saito, S.; Miyazawa, Y.; Umezawa, T.; Shimada, Y.; Min, Y. K.; Mizutani, M.; Hirai, N.; Shinozaki, K.; Yoshida, S.; Asami, T. *Bioorg. Med. Chem.* **2005**, *13*, 4491.

8.   Saito, S.; Okamoto, M.; Shinoda, S.; Kushiro, T.; Koshiba, T.; Kamiya, Y.; Hirai, N.; Todoroki, Y.; Sakata, K.; Nambara, E.; Mizutani, M. *Biosci. Biotechnol. Biochem.* **2006**, *70*, 1731.

9.   Saito, S.; Hirai, N.; Matsumoto, C.; Ohigashi, H.; Ohta, D.; Sakata, K.; Mizutani, M. *Plant Physiol.* **2004**, *134*, 1439.

10.   Kushiro, T.; Okamoto, M.; Nakabayashi, K.; Yamagishi, K.; Kitamura, S.; Asami, T.; Hirai, N.; Koshiba, T.; Kamiya, Y.; Nambara, E. *ENBO J.* **2004**, *23*, 1647.

11.   Poulos, T. L.; Johnson, E. F. In *Cytochrome P450: Structure, Mechanism, and Biochemistry*, 3rd ed.; Ortiz de Montellano, P. R. Ed.; Kluwer Academic/Plenum Publishers, New York, 2005; pp 87-114.

12.   Schuler, M. A. *Critical Rev. in Plant Sciences* **1996**, *15*, 235.

13.   Ueno, K.; Araki, Y.; Hirai, N.; Saito, S.; Mizutani, M.; Sakata, K.; Todoroki, Y. *Bioorg. Med. Chem.* **2005**, *13*, 3359.

14.   Todoroki, Y.; Kobayashi, K.; Yoneyama, H.; Hiramatsu, S.; Jin, M.-H.; Watanabe, B.; Mizutani, M., Hirai, N. *Bioorg. Med. Chem.* **2008**, *16*, 3141.

15.   Wang, Z.; Silverman, R. B. *Bioorg. Med. Chem.* **2006**, *14*, 2242 and references cited therein.

16.   Saito, J.; Kurahashi, Y.; Goto, T.; Yamaguchi, N. (Nihon Tokushu Noyaku Seizo K. K.). Eur. Pat. Appl. EP185987, 1986.

17.   Nambara, E.; Marion-Poll, A. *Annu. Rev. Plant Biol.* **2005**, *56*, 165.

18.   See supplementary data in ref. 14.

19.   Amino, Y.; Eto, H.; Eguchi, C. *Chem. Pharm. Bull.* **1989**, *37*, 1481.

20.   Omura, T.; Sato, R. *J. Biol. Chem.* **1964**, *239*, 2370.

21.   *SigmaPlot 10*; Systat Software, Inc.: Richmond CA, 2006.

22.   *CAChe, 3.11*; Oxford Molecular Ltd.: London, 1998.

23.   *Gaussian 03 Revision D.01*; Gaussian, Inc.: Wallingford CT, 2004.

Table, Figure, and Scheme legends

Table 1.   Inhibitory activity of conformationally restricted analogues of UNI against recombinant CYP707A3 and rice seedling elongation.

Figure 1.   Uniconazole (UNI) is a potent inhibitor of ABA 8'-hydroxylase and *ent*-kaurene oxidase.

Figure 2.   Four conformers **A–D** generated by bond rotations of C2–N1" and C2–C3 in UNI.

Figure 3.   Conformationally restricted analogues of UNI.

Figure 4.   3D structures of *S*-UNI (crystalline and theoretical) and *S*-**1** (theoretical).

Figure 5.   Competitive inhibition of ABA 8'-hydroxylase by 3*R*-**5**. Assays contained *S*-ABA (●) or *S*-ABA and 0.5 µM 3*R*-**5** (○). The inset is a double-reciprocal plot for the same data. The same mode of inhibition was observed for 3*S*-**5** and *S*- and *R*-**9** (data not shown).

Figure 6.   Inhibitory effect of 3*S*- and 3*R*-**5** and *S*-UNI on rice seedling growth.

Figure 7.   Effect of 3*R*-Abz-F1 (**5**) and *S*-UNI on stomatal aperture of apple seedlings: control (●), 10 µM 3*R*-Abz-F1 (○), and 10 µM *S*-UNI (▼). Similar changes were observed at 50 and 100 µM (data not shown). Dashed line shows changes in water potential of vermiculite in which apple seedlings were cultivated.

Figure 8.   Drought tolerance of apple seedlings treated with (a) 3*R*-Abz-F1 (**5**) and (b) *S*-UNI.

Figure 9. Drought tolerance of apple seedlings treated with distilled water (left), 10 μM of 3*R*-Abz-F1 (**5**) (center), and 10 μM of *S*-UNI (right).

Scheme 1. Synthesis of *S*-**1**. Reagents and conditions: ClCOOCCl$_3$, pyridine, dry CH$_2$Cl$_2$, 0 °C, 98%. *R*-**1** and racemic **1** were synthesized by the same scheme from *R*-UNI and racemic UNI, respectively.

Scheme 2. Synthesis of **2** and **3**. Reagents and conditions: (i) LiAlH$_4$, dry Et$_2$O, 0 °C, 47% (**2**); (ii) Et$_3$SiH, BF$_3$·Et$_2$O, rt, 13%.

Scheme 3. Synthesis of **4**, **5**, and **6**. Reagents and conditions: (i) ClCOOCCl$_3$, pyridine, dry CH$_2$Cl$_2$, 0 °C, 94%; (ii) LiAlH$_4$, dry Et$_2$O, 0 °C, 38% (**5**), 24% (**18**); (iii) ZnCl$_2$, dry 1,2-dichloroethane, 100 °C, 51%; (iv) UV 365 nm, EtOAc, rt, 32%.

Scheme 4. Synthesis of **7** and **9**. Reagents and conditions: (i) see ref. 16; (ii) NaH, 1-bromo-3,3-dimethyl-2-butanone, dry Et$_2$O, 0 °C, 9%; (iii) *p*-chlorobenzaldehyde, K$_2$CO$_3$, Ac$_2$O, 100 °C, 62%; (iv) UV 365 nm, EtOAc, rt, 63%; (v) NaBH$_4$, MeOH, 0 °C to rt, 49%; (vi) 1M HCl, EtOH-H$_2$O, rt, 89%; (vii) MnO$_2$, acetone, rt, 35% (**7**); (viii) ZnCl$_2$, dry CH$_2$Cl$_2$, rt, 27%.

Table 1. Inhibitory activity of conformationally restricted analogues of UNI against recombinant CYP707A3 and rice seedling elongation.

Compound	Structural properties[a]			CYP707A3		rice
	azole	bridge	conf.	Inhibition[b] (%)	K_I (nM)	IC$_{50}$[c] (μM)
S-UNI	Trz		**A/B**	100	10	0.18
R-UNI	Trz		**A/B**	79±1	1450	7.8
1	Trz	Lon	**B**	14±5	NM[d]	2.3
S-**1**	Trz	Lon	**B**	10±7	NM	1.3
R-**1**	Trz	Lon	**B**	27±24	NM	46
2	Trz	Lol	**B**	69±7	NM	3.2
3	Trz	Ether	**B**	31±10	NM	78
4	Imz	Lon	**B**	35±8	NM	NI[e]
5 (Abz-F1)	Imz	Lol	**B**	91±5	NM	NI
3*S*-**5**	Imz	Lol	**B**	96±4	970	NI
3*R*-**5**	Imz	Lol	**B**	95±7	420	NI
6	Imz	Ether	**B**	13±6	NM	28
7	Imz	Lon	**A**	52±2	NM	58
9	Imz	Ether	**A**	100	NM	9.0
S-**9**	Imz	Ether	**A**	100	160	8.2
R-**9**	Imz	Ether	**A**	87±3	520	12

[a] azole, type of azole (Trz, triazole; Imz, imidazole); bridge, bridging moiety (Lon, lactone; Lol, lactol; Ether, cyclic ether); conf., type of conformation (see Figs. 2 and 3).

[b] Inhibition ratio of compounds (10 μM) in the 8'-hydroxylation of ABA (5 μM) (average of at least three sets of experiments).

[c] The concentration for 50% inhibition (average of at least two sets of experiments).

[d] Not measured.

[e] No significant inhibition even at 100 μM (max concentration tested).

ABA catabolism

ABA 8'-hydroxylase
(CYP707A)

S-(+)-ABA

8'-hydroxy-ABA

5'
4'
6'
3'
1'
2'
3
2" 1" 2 1
N—N
3" 4" 5"
N

S-(+)-UNI

ent-kaurene

ent-kaurene oxidase
(CYP701A)

GA biosynthesis

ent-kaurenoic acid
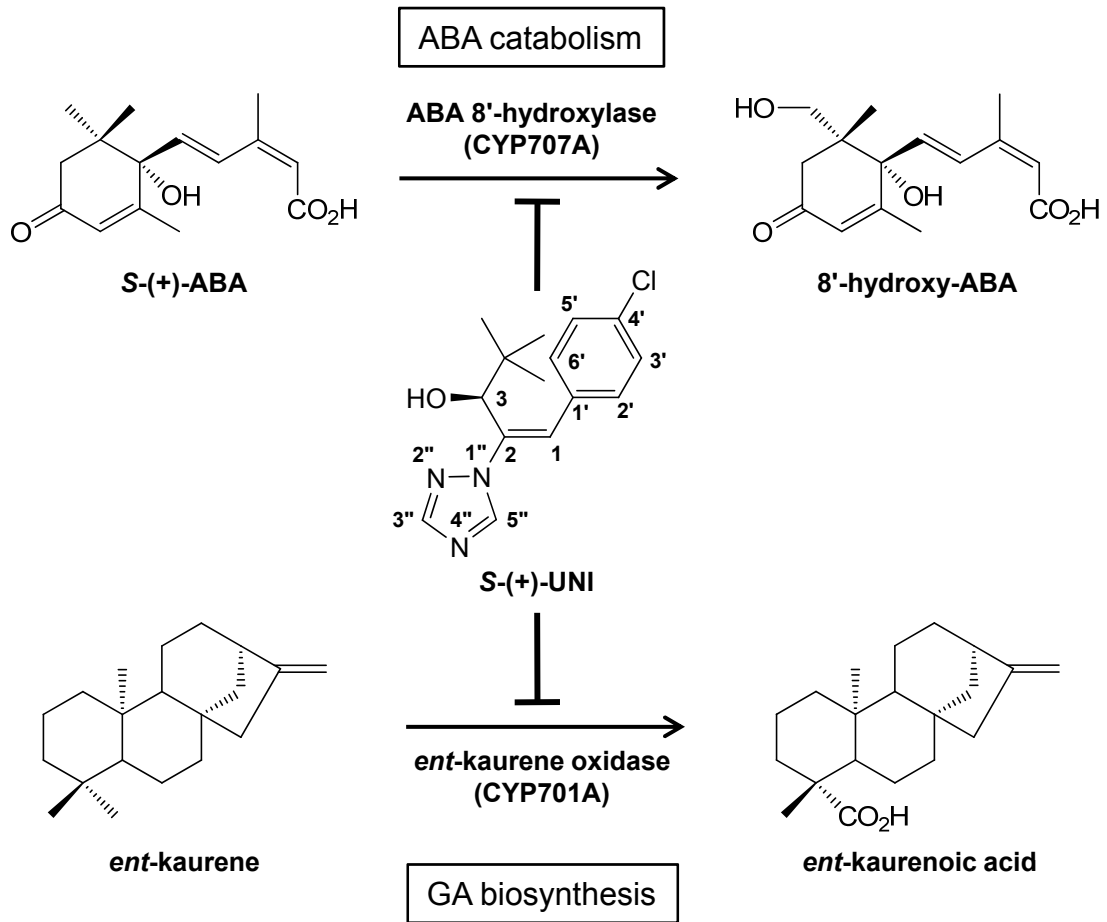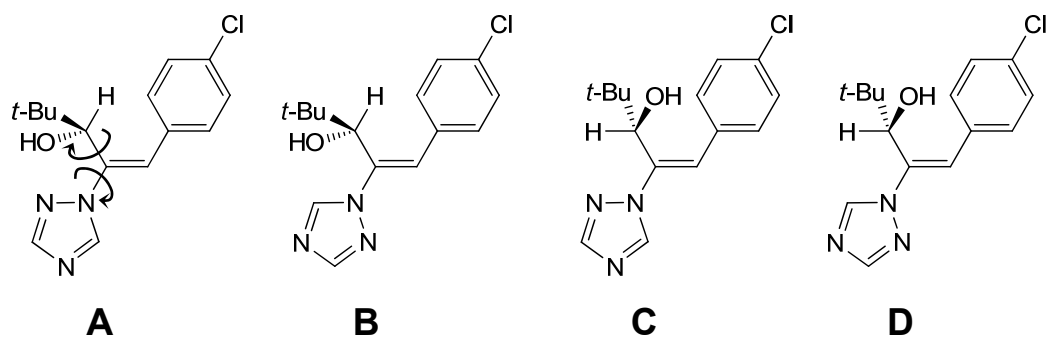
Figure 1

Figure 2

B-type restriction
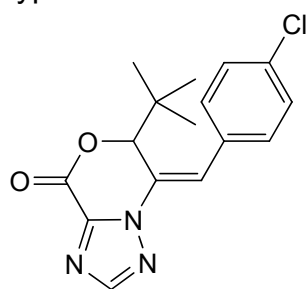
1
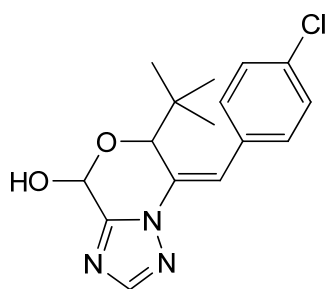
2
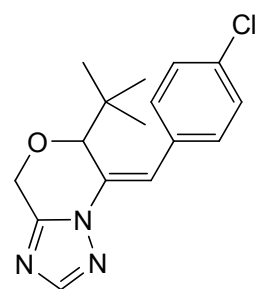
3
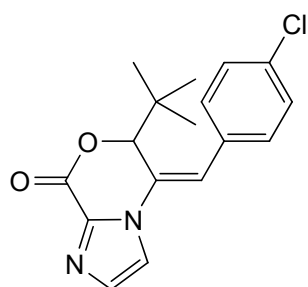
4
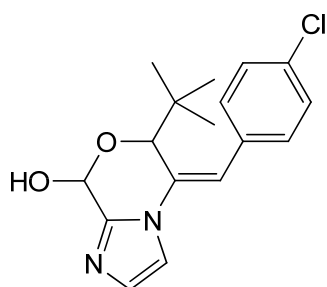
5
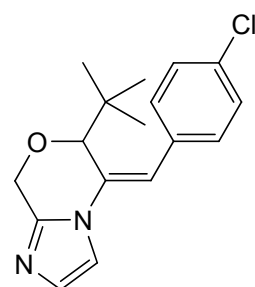
6

A-type restriction
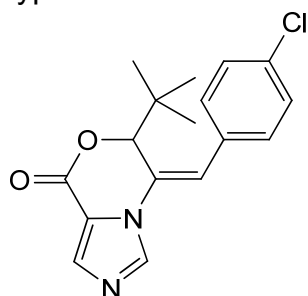
7
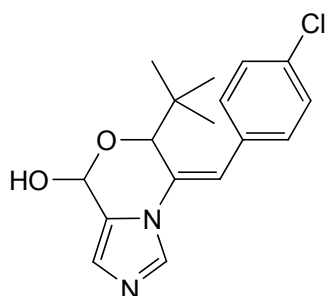
8
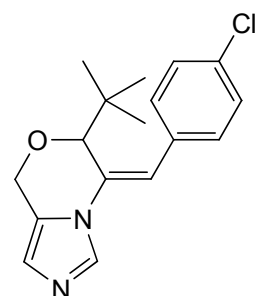
9

Figure 3
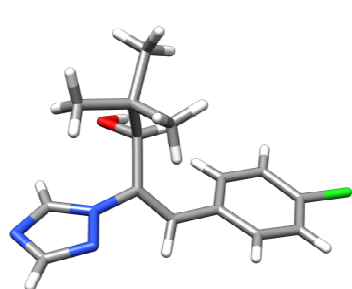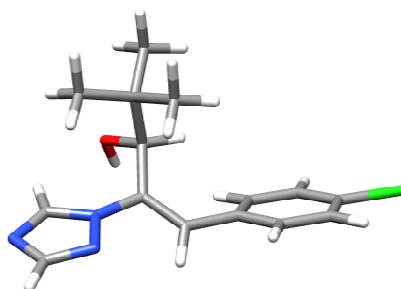
crystalline   theoretical   theoretical

B-type form of *S*-UNI   *S*-**1**

Figure 4

Figure 5

3S-**5**

3R-**5**

S-UNI

| 0 | 0.3 | 1 | 3 | 10 | 30 | 100 |

concentration [μM]

Figure 6

Figure 7

a

control   10   50   100

conc. of 3*R*-Abz-F1 (**5**) [μM]

b

control   10   50   100

conc. of *S*-UNI [μM]
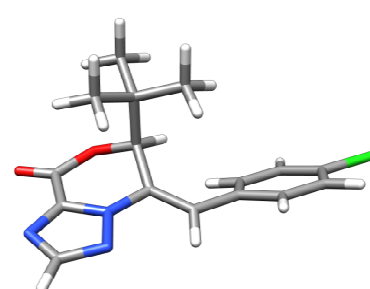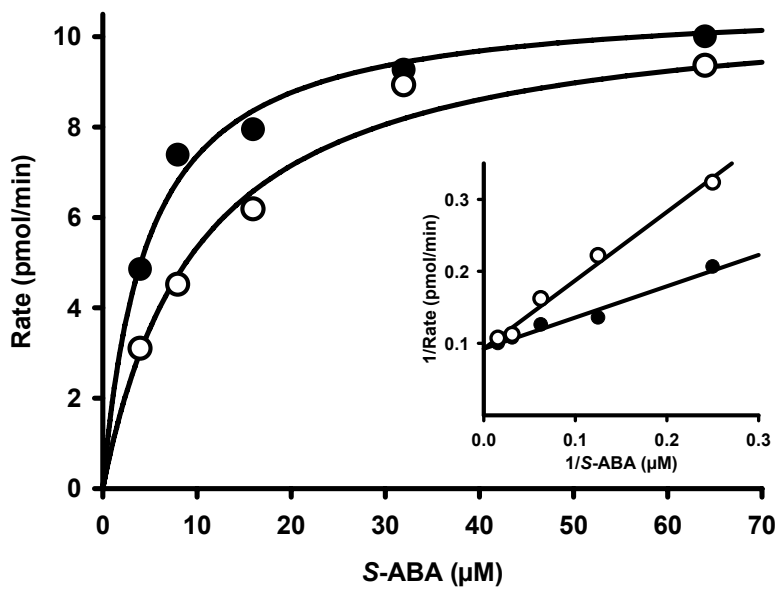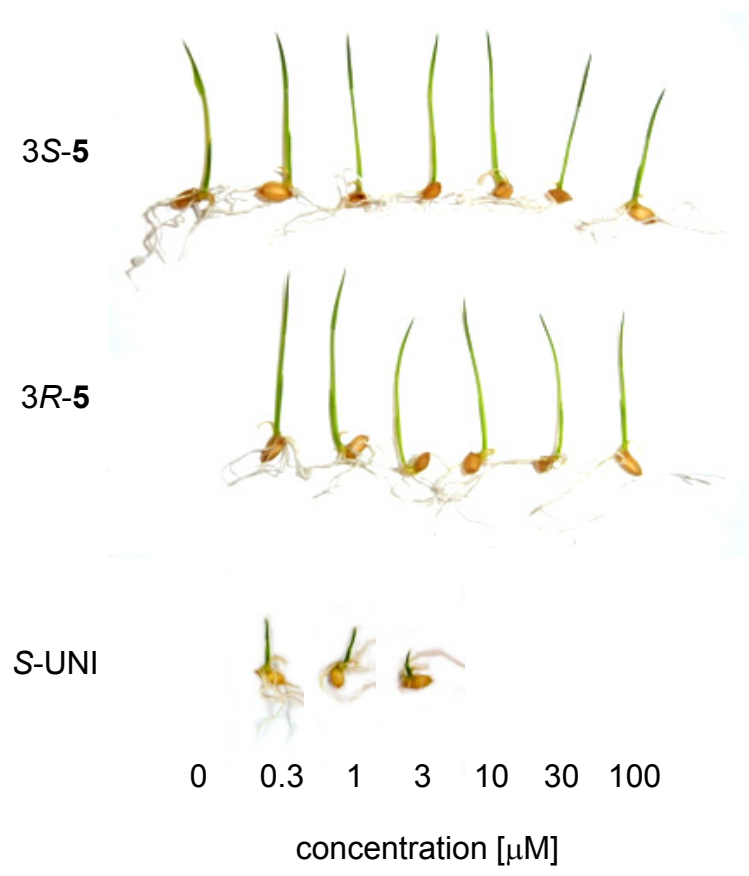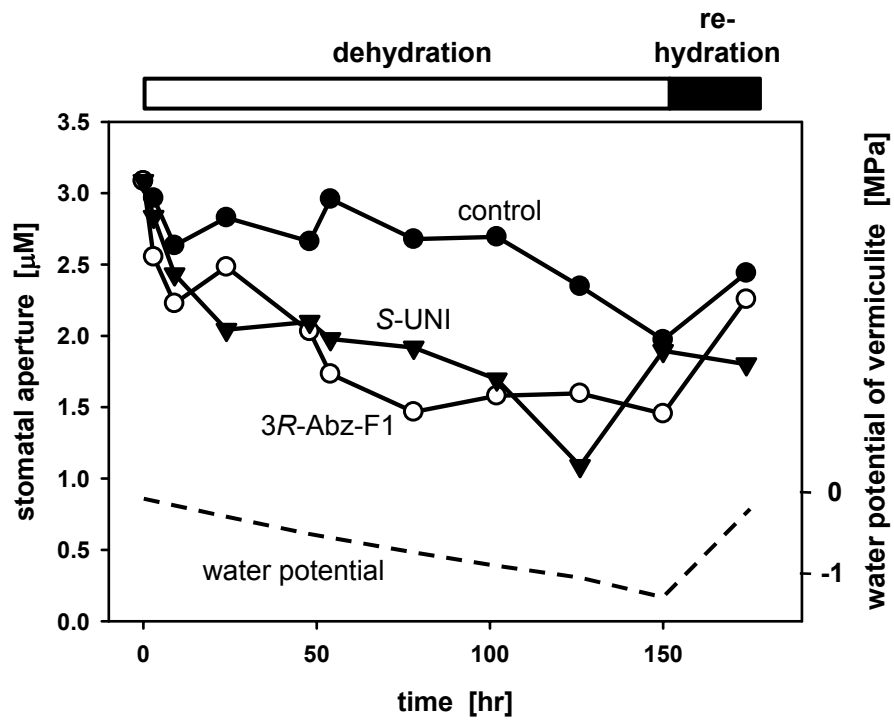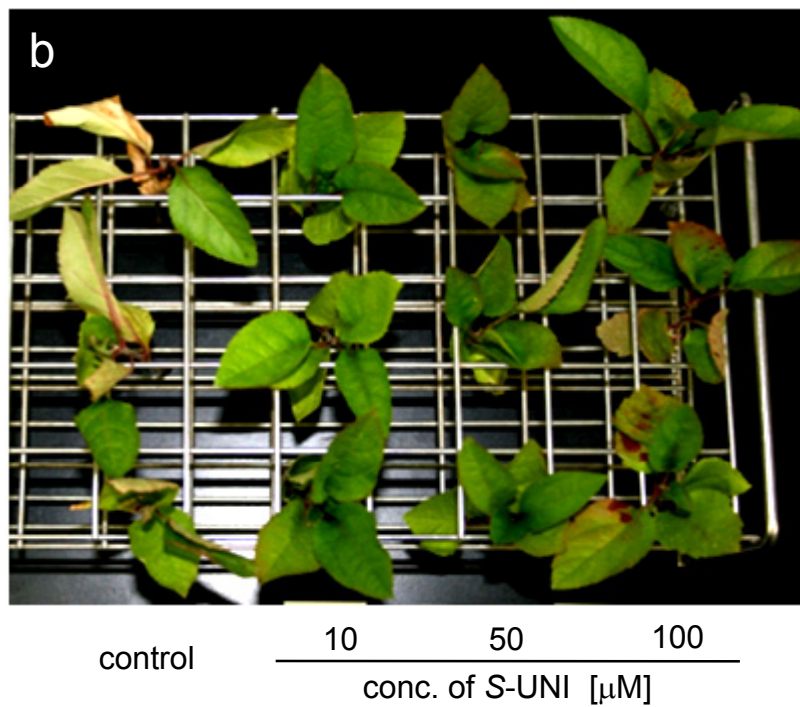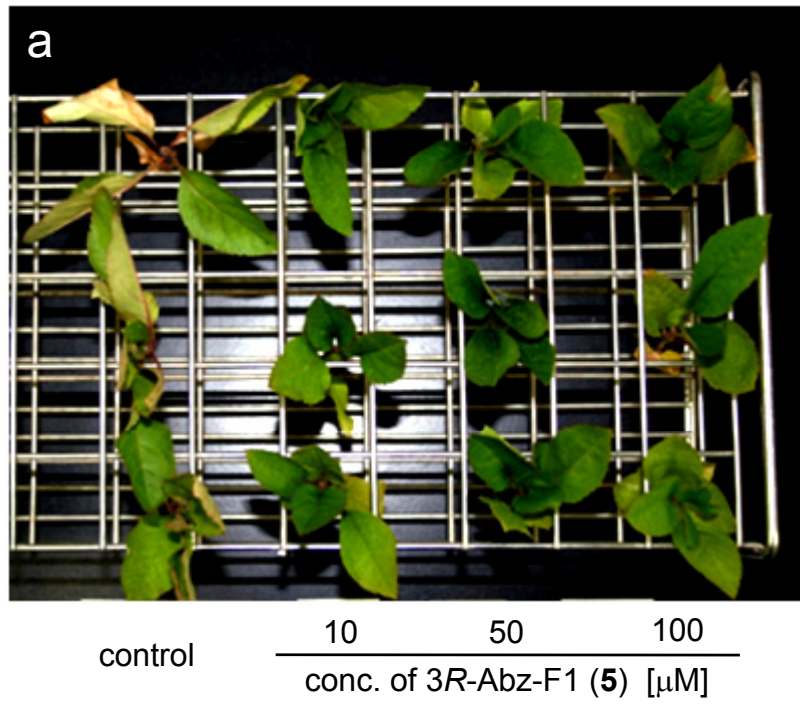
Figure 8

control   3*R*-Abz-F1 (**5**)   *S*-UNI

Figure 9

S-UNI $\longrightarrow$

S-**1**

Scheme 1

1 $\xrightarrow{\text{i}}$ 2 +

10

ii ↓

3

Scheme 2

11 $\xrightarrow{\text{i}}$ **4** $\xrightarrow{\text{ii}}$ **5** + **12** $\xrightarrow{\text{iii}}$ **6Z** $\xrightarrow{\text{iv}}$ **6**
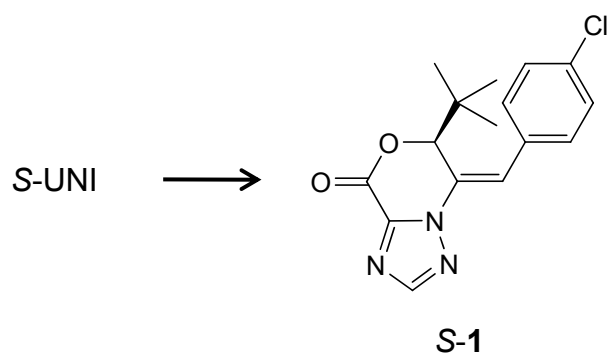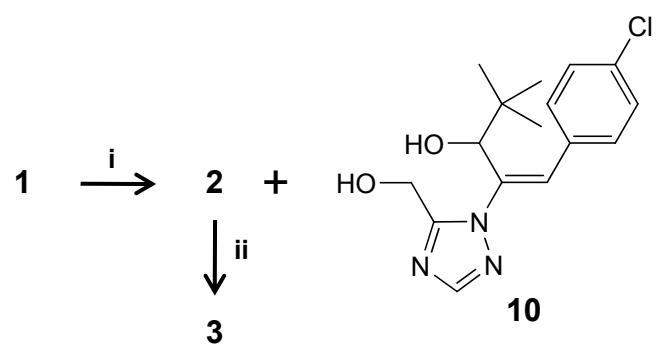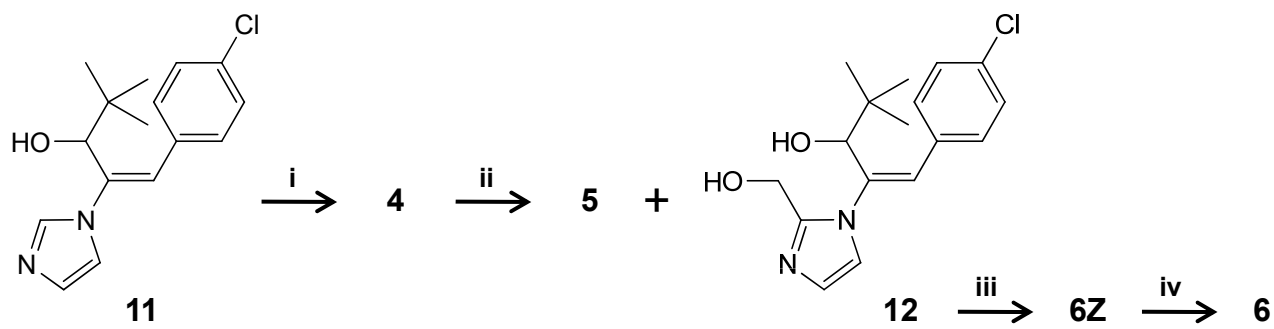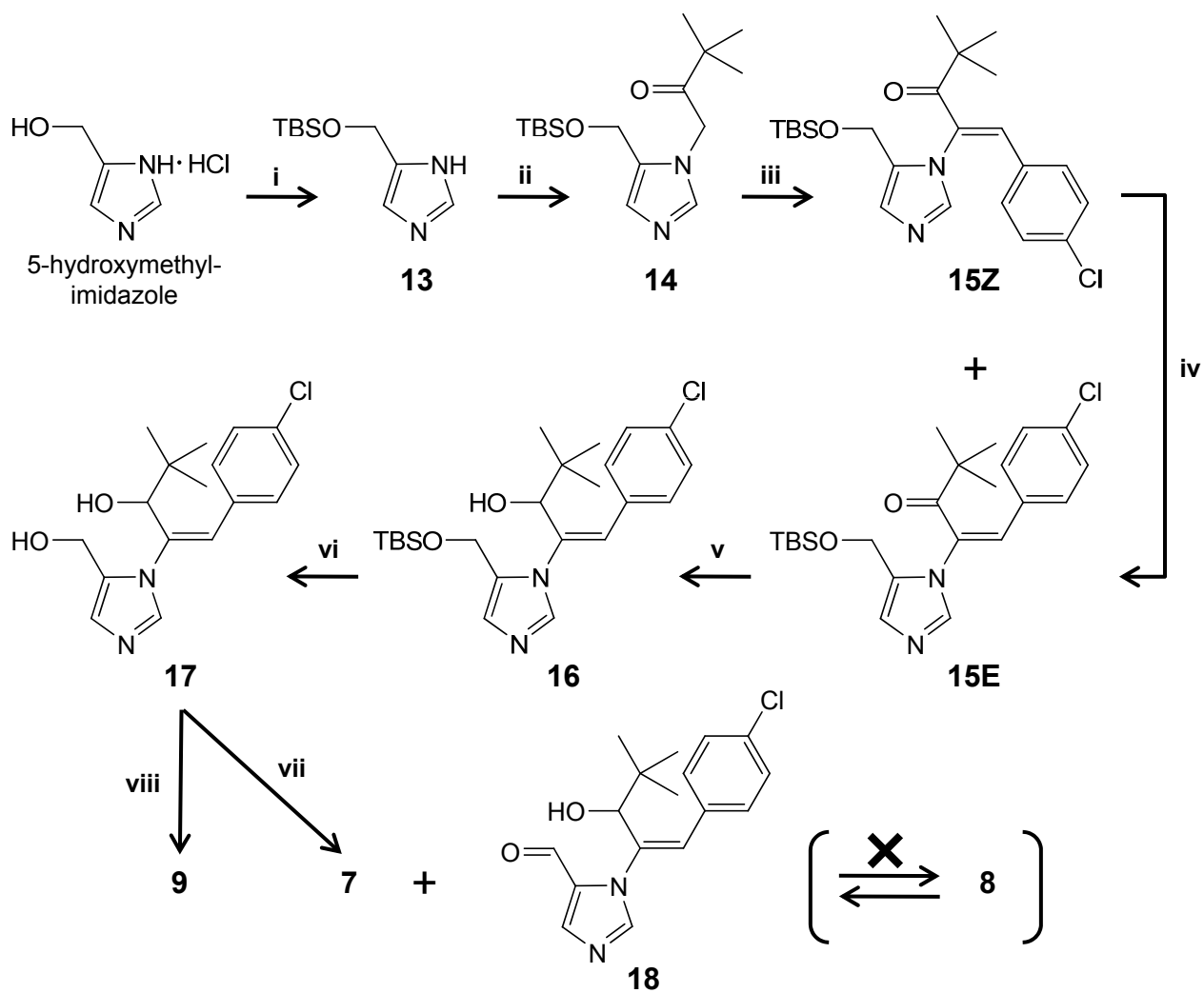
Scheme 3

Scheme 4

Abscinazole-F1, a conformationally restricted analogue of the plant growth retardant uniconazole and an inhibitor of ABA 8'-hydroxylase CYP707A with no growth-retardant effect

Yasushi Todoroki,[a,*] Kyotaro Kobayashi,[a] Minaho Shirakura,[a] Hikaru Aoyama,[a] Kokichi Takatori,[a] Hataitip Nimitkeatkai,[b] Mei-Hong Jin,[a] Saori Hiramatsu,[a] Kotomi Ueno,[c,†] Satoru Kondo,[b] Masaharu Mizutani,[d,‡] Nobuhiro Hirai[e]

Supplementary data

Determination of the absolute configuration of optically pure **9**, determination of the *E*- and *Z*-isomers of conformationally restricted UNI analogues, and ^{1}H NMR spectra of new compounds which were used in the enzymatical and biological assays

1. Determination of the absolute configuration of optically pure 9

1.1. Geometry optimization of 9

The geometry of **9** was generated and minimized using MM3 built into CAChe 3.11.   The MM3-minimized structure was fully optimized with density functional theory, using the Becke three parameter hybrid functional (B3LYP) method and the 6-31G(d) basis set in Gaussian 03, followed by a calculation of the harmonic vibrational frequencies at 298 K at the same level.   The single point energy was calculated with B3LYP/6-311++G(2df,2p) level of theory.   The zero-point energy was scaled by 0.9804.

S-**9**
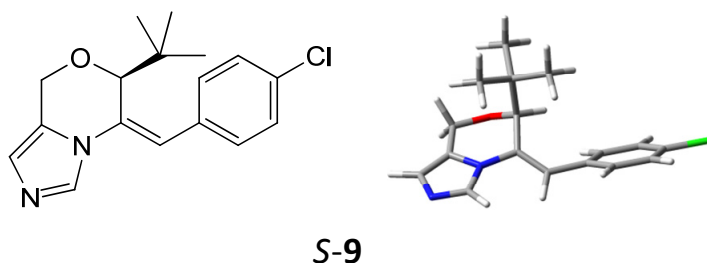
| B3LYP/6−31G(d) | | B3LYP/6−311++G(2df,2p) | total energy |
ZPE, hartrees	ZPE x 0.9804, hartrees	SPE, hartrees	hartrees
0.330349	0.323874	−1304.44352790	−1304.11965374

Figure S1.   Structure of *S*-**9**.

1.2. TDDFT calculations of CD of 9

The electronic circular dichroism (ECD) calculations were carried out by means of TDDFT (TD=NStates=30) methods with the B3LYP/6-31G(d) level of theory, as available within Gaussian 03 (Figure S2). Both velocity and length formalism have been used in ECD calculations. The CD spectra were simulated by overlapping Gaussian functions for each transition according to

$$\Delta\varepsilon(E) = \frac{1}{2.297 \times 10^{-39}} \frac{1}{\sqrt{2\pi}\sigma} \sum_{i}^{A} \Delta E_i R_i \exp\left[-\left(\frac{E - \Delta E_i}{2\sigma}\right)^2\right]$$

where σ is the width of the band at $1/e$ height, and ΔE_i and R_i are the excitation energies and rotatory strengths for transition i, respectively. A σ value of 0.2 eV was used. [ref.: Diedrich, C.; Grimme, S. *J. Phys. Chem. A* **2003**, *107*, 2524.]
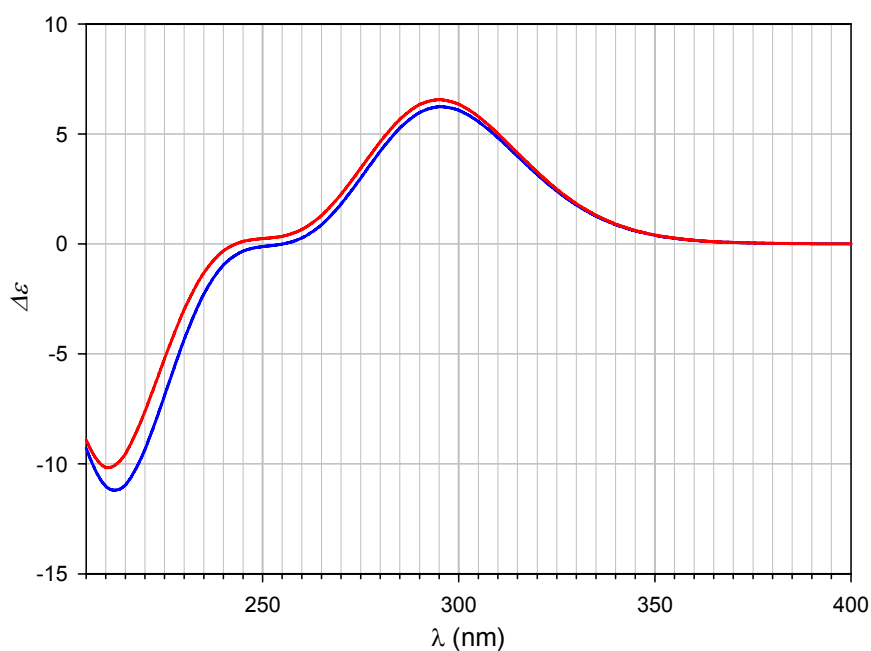
Figure S2. Theoretical CD spectra of *S*-**9**. The theoretical curves were obtained at the TDDFT/B3LYP/6-31G* level, taking into account the 30 lowest energy transitions and assuming a Gaussian distribution with σ = 0.2 eV. Blue line, calculated in the velocity formalism; red line, calculated in the length formalism

1.3. Experimental CD spectra of optically pure 9

Circular dichroism (CD) spectra were recorded with a Jasco J-805 spectrophotometer. (+)-**9**: CD λmax (MeOH) nm ($\Delta\varepsilon$): 275 (+7.2), 241 (0), 216 (−19.4). (−)-**9**: CD λmax (MeOH) nm ($\Delta\varepsilon$): 275 (−7.1), 244 (0), 214 (+21.0).
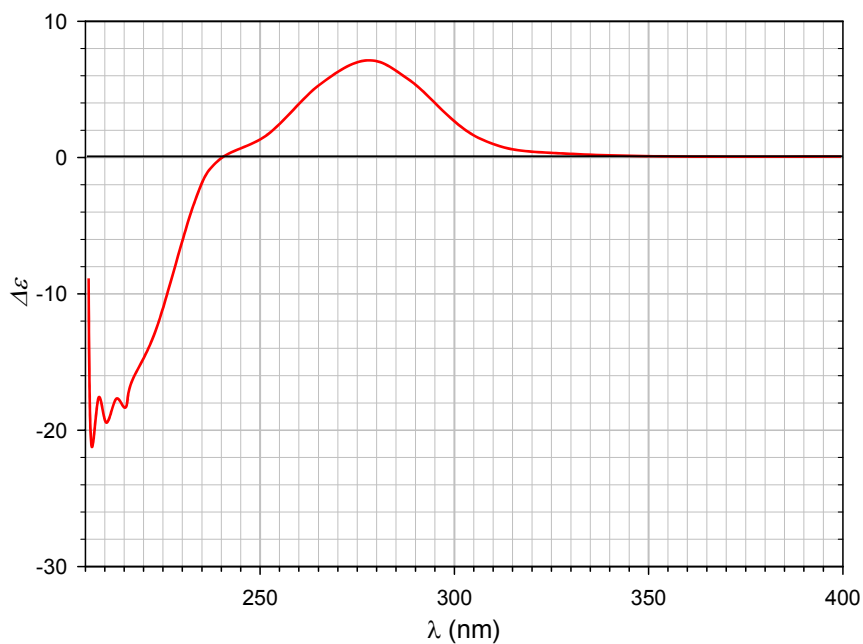
Figure S3. Experimental CD spectrum of (+)-**9**.

1.4. Comparison of theoretical and experimental CD spectra of 9

Figure S4 shows that (+)-**9** is *S*-**9**.
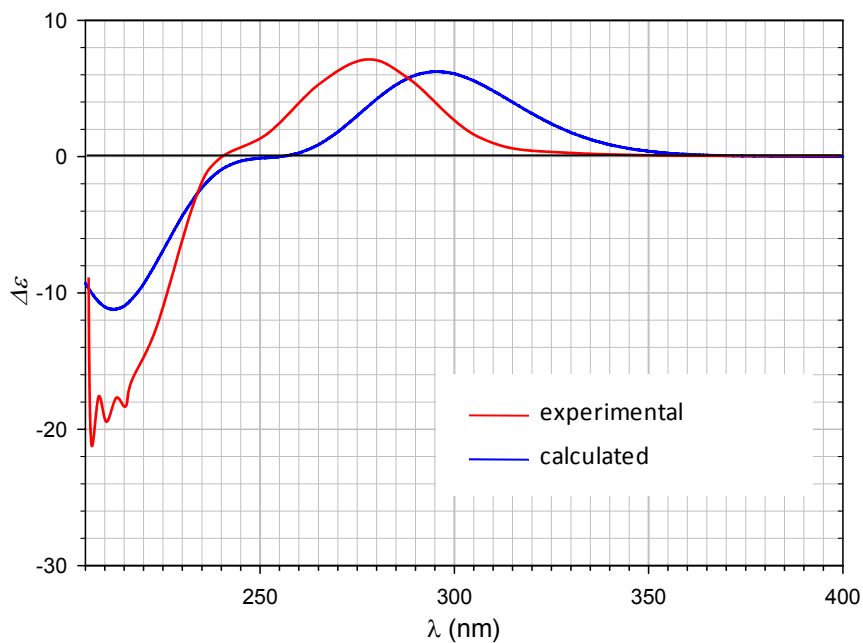
Figure S4. Comparison of theoretical CD spectrum (velocity) of *S*-**9** and experimental CD spectrum of (+)-**9**.

2. Determination of the *E*- and *Z*-iomers of UNI analogues

Because the *E*-isomer has the plane structure and the H-1 is *syn* to the azole ring, the H-1 is deshielded by two aromatic rings, 4-Cl-Ph and Az. On the other hand, because the Z-isomer has the bent structure and the H-1 is *anti* to the azole ring, the H-1 is deshielded by only 4-Cl-Ph. Therefore, the H-1 of the *E*-isomer is shifted to the lower field compared to that the *Z*-isomer.
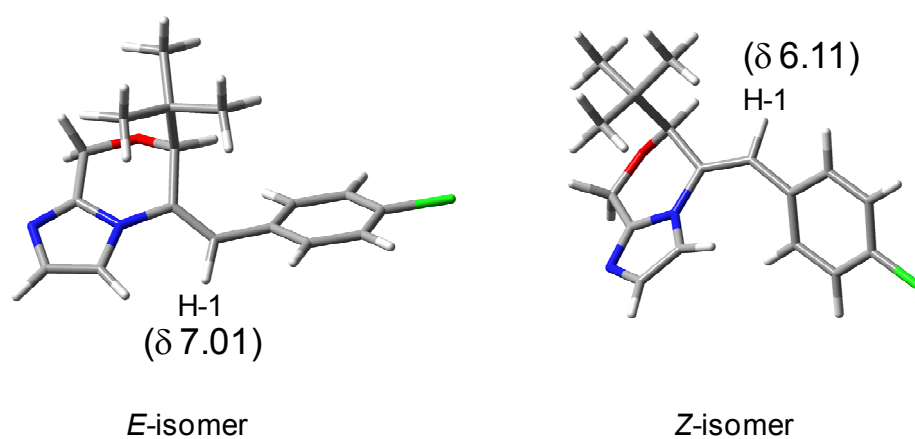
E-isomer   *Z*-isomer

Figure S5. The 3D structures of the *E*- and *Z*-isomers of **6**. The geometry was fully optimized with density functional theory, using the Becke three parameter hybrid functional (B3LYP) method and the 6-31G(d) basis set in Gaussian 03.

3. ^{1}H NMR spectra of new compounds which were used in the enzymatical and biological assays

Compound *S*-1
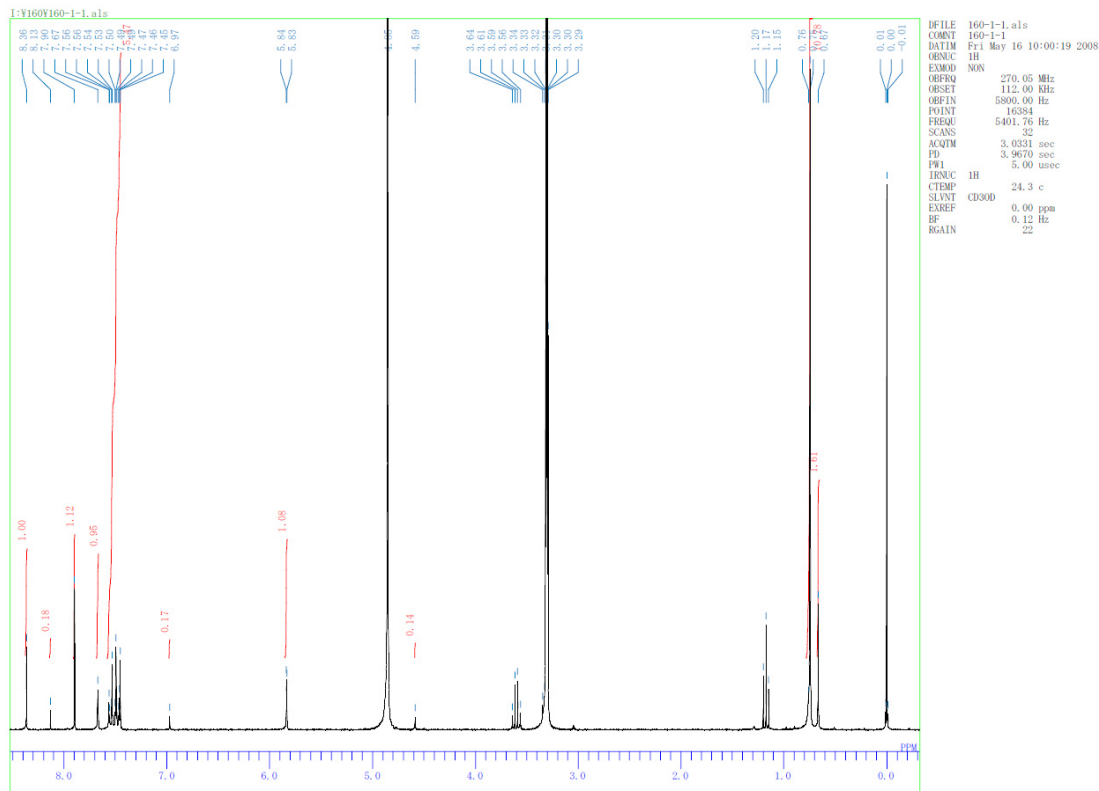
Compound *R*-1
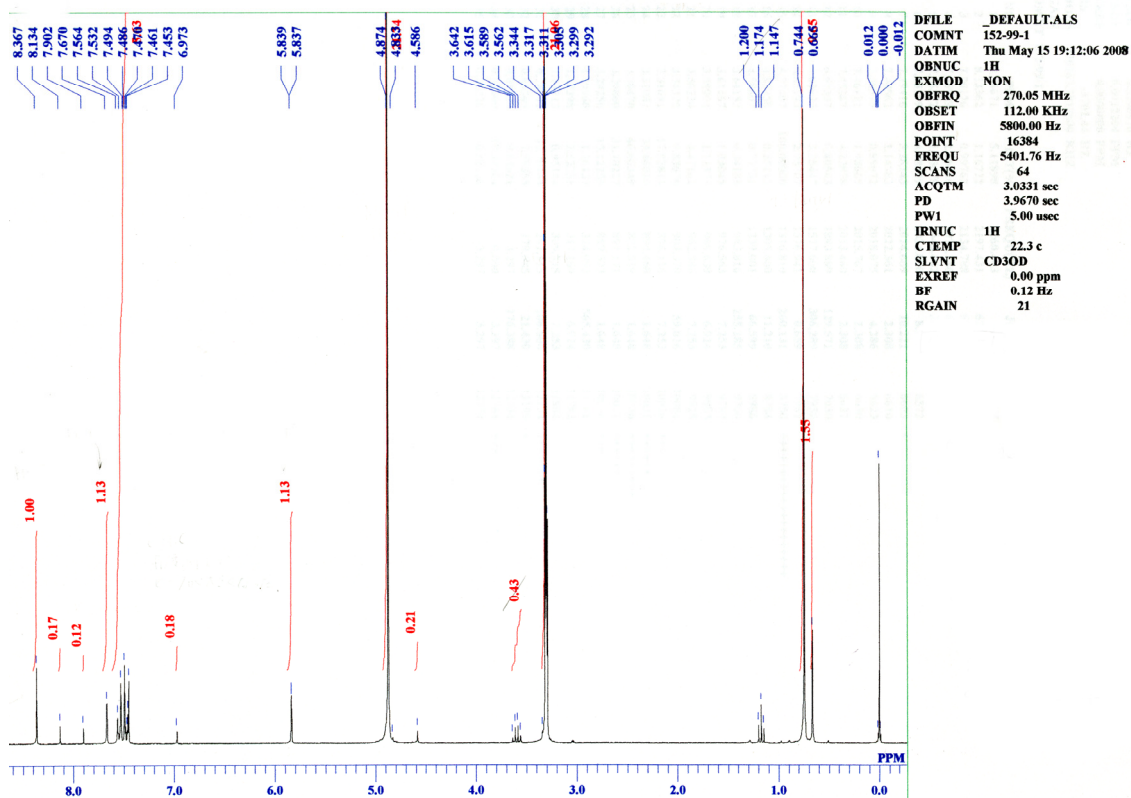
Compound 2
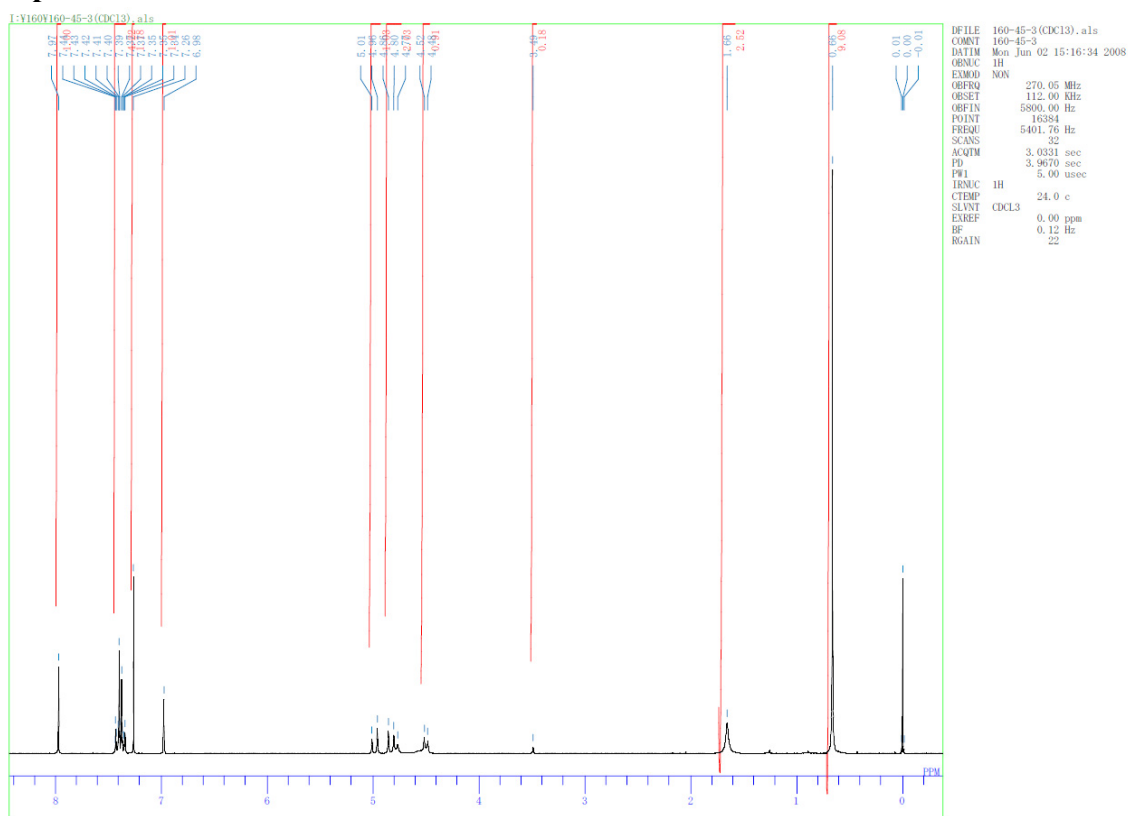
Compound 3
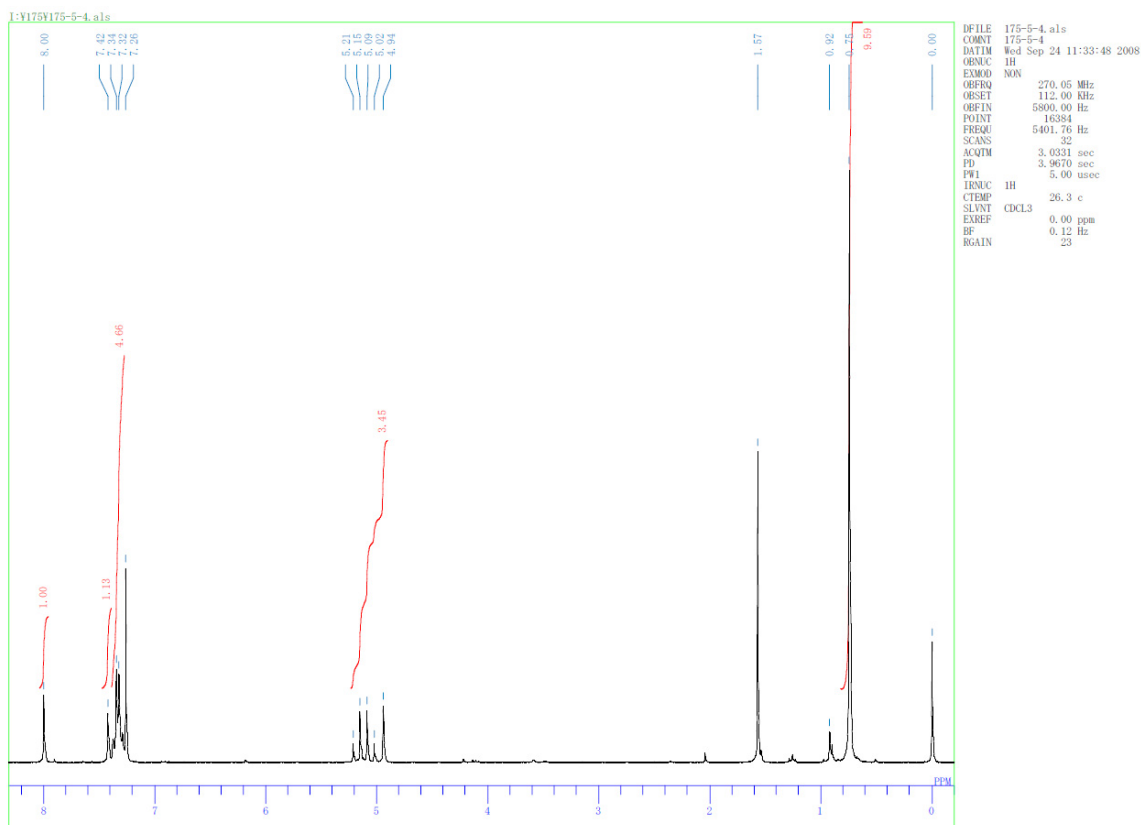
Compound 4
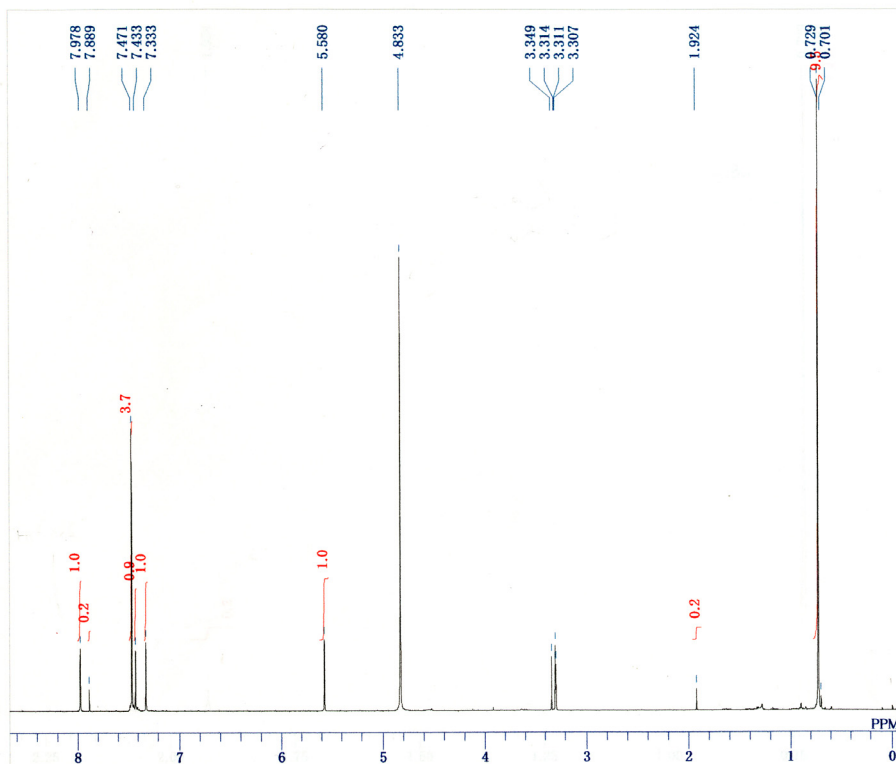
DFILE   174191-h.als
COMNT   174-19-1
DATIM   Wed Oct 29 09:24:05 2008
OBNUC   1H
EXMOD   non
OBFRQ   500.00 MHz
OBSET   0.00 KHz
OBFIN   162160.00 Hz
POINT   32768
FREQU   10000.00 Hz
SCANS   4
ACQTM   3.2768 sec
PD   3.7230 sec
PW1   2.95 usec
IRNUC   1H
CTEMP   28.1 c
SLVNT   CD3OD
EXREF   0.00 ppm
BF   0.12 Hz
RGAIN   16

Compound 5
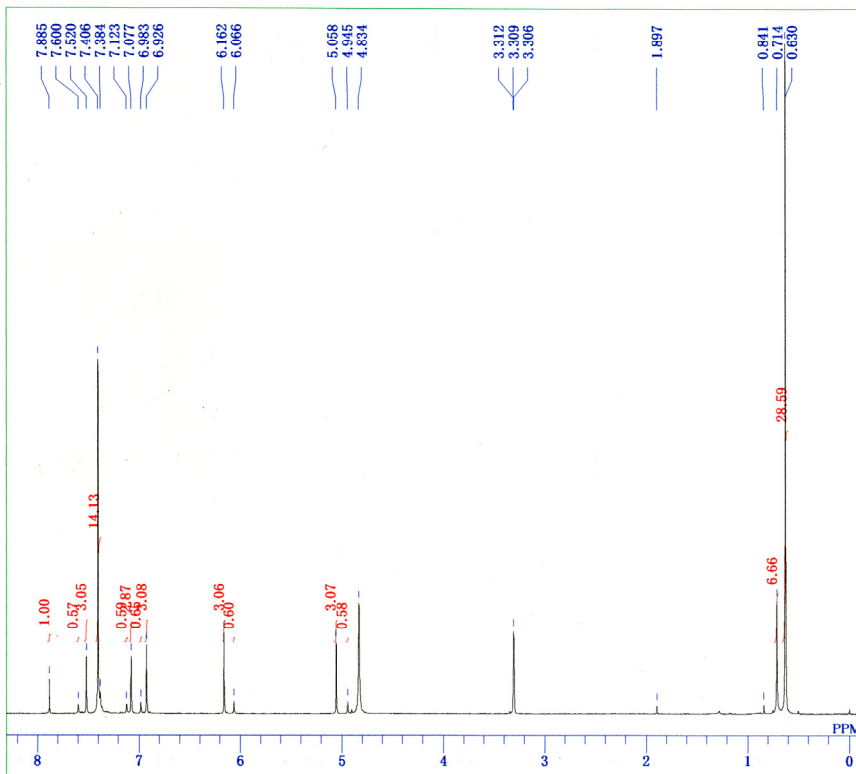
DFILE   179191-h.als
COMNT   179-19-1
DATIM   Mon Jan 19 10:57:01 2009
OBNUC   1H
EXMOD   non
OBFRQ   500.00 MHz
OBSET   0.00 KHz
OBFIN   162160.00 Hz
POINT   32768
FREQU   10000.00 Hz
SCANS   8
ACQTM   3.2768 sec
PD   3.7230 sec
PW1   2.95 usec
IRNUC   1H
CTEMP   28.0 c
SLVNT   CD3OD
EXREF   0.00 ppm
BF   0.12 Hz
RGAIN   16

Compound *3S*-5
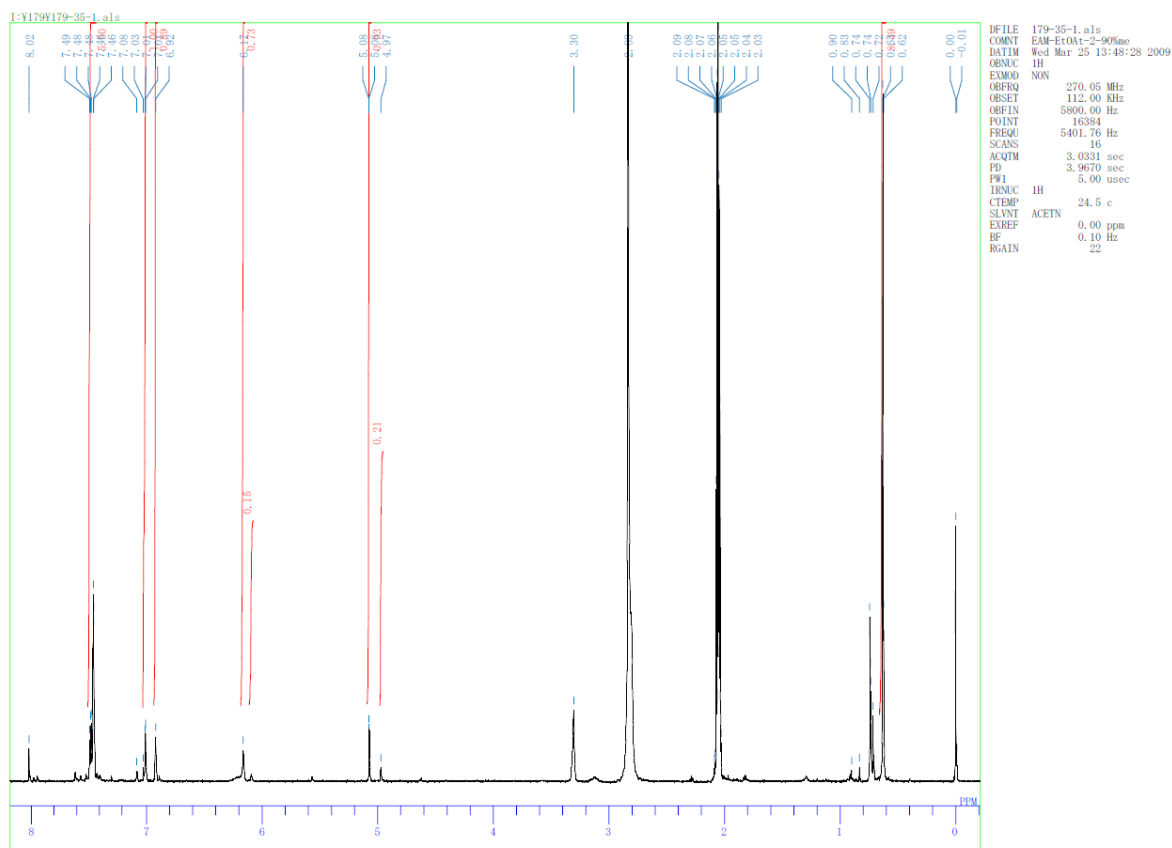
Compound *3R*-5
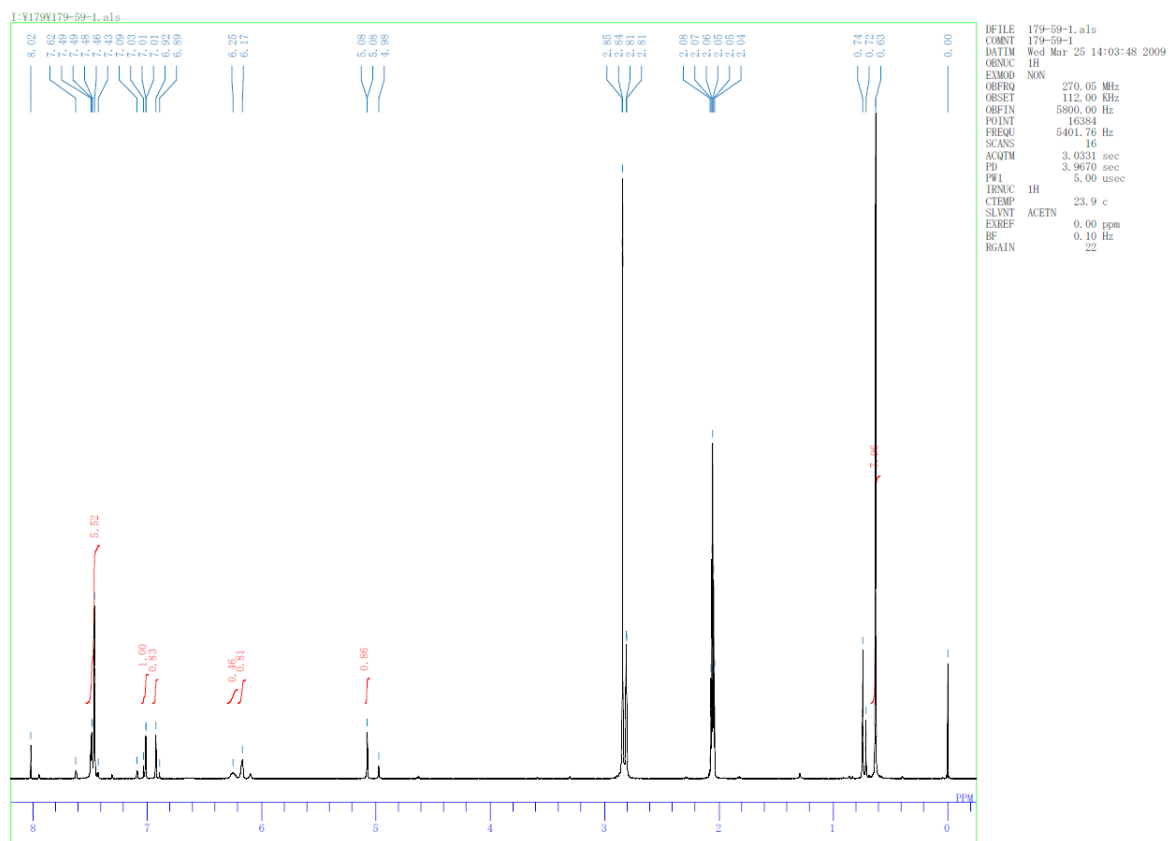
Compound 6
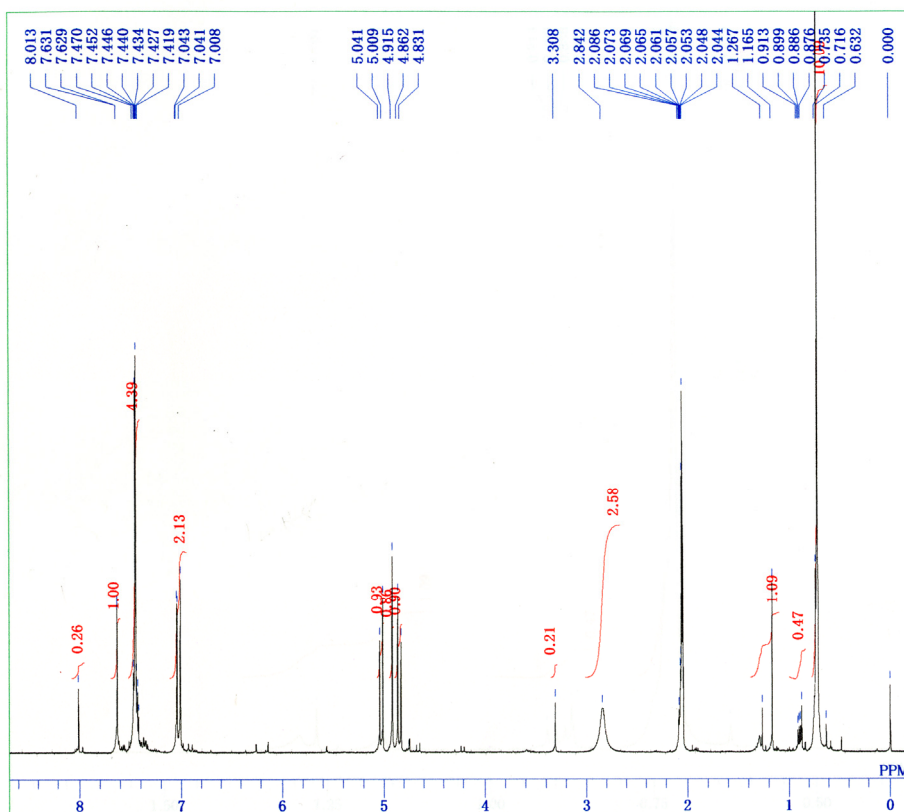
DFILE   174471-h.als
COMNT   174-47-1
DATIM   Mon Jan 19 17:49:32 2009
OBNUC   1H
EXMOD   non
OBFRQ   500.00 MHz
OBSET   0.00 KHz
OBFIN   162160.00 Hz
POINT   32768
FREQU   10000.00 Hz
SCANS   8
ACQTM   3.2768 sec
PD   3.7230 sec
PW1   2.95 usec
IRNUC   1H
CTEMP   28.0 c
SLVNT   ACETN
EXREF   0.00 ppm
BF   0.12 Hz
RGAIN   20

Compound 7
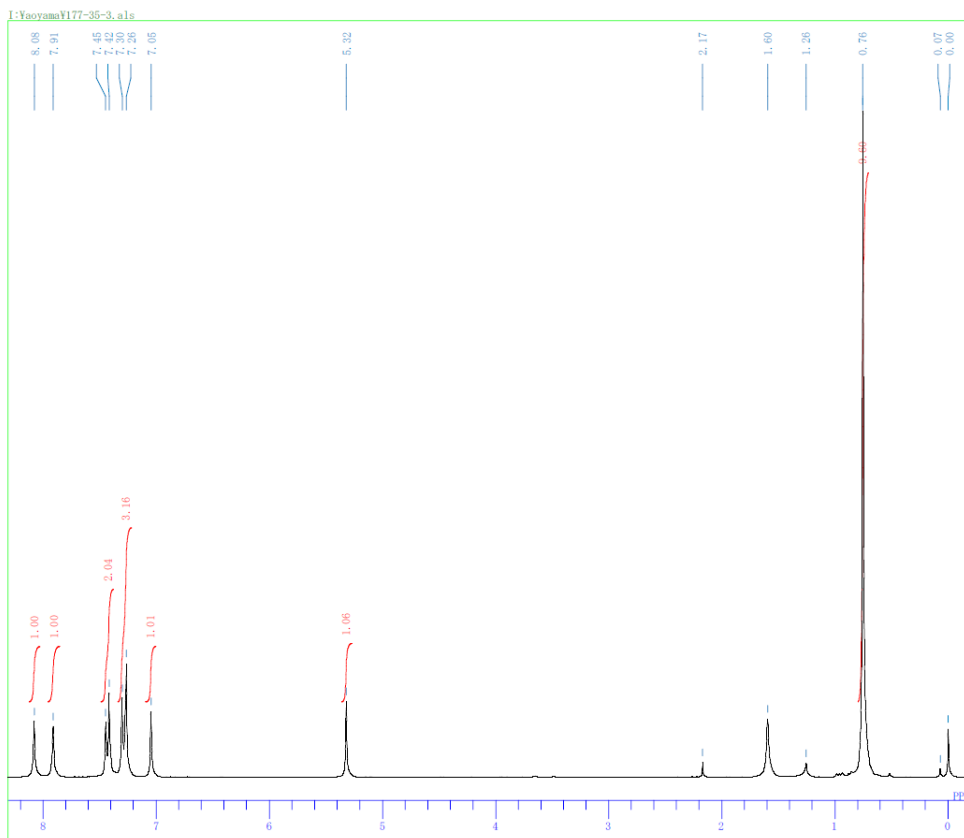
DFILE   177-35-3.als
COMNT   177-35-3
DATIM   Wed Dec 03 20:47:34 2008
OBNUC   1H
EXMOD   NON
OBFRQ   270.05 MHz
OBSET   112.00 KHz
OBFIN   5800.00 Hz
POINT   16384
FREQU   5401.76 Hz
SCANS   64
ACQTM   3.0331 sec
PD   3.9670 sec
PW1   5.00 usec
IRNUC   1H
CTEMP   26.5 c
SLVNT   CDCL3
EXREF   0.00 ppm
BF   1.50 Hz
RGAIN   21

Compound 9
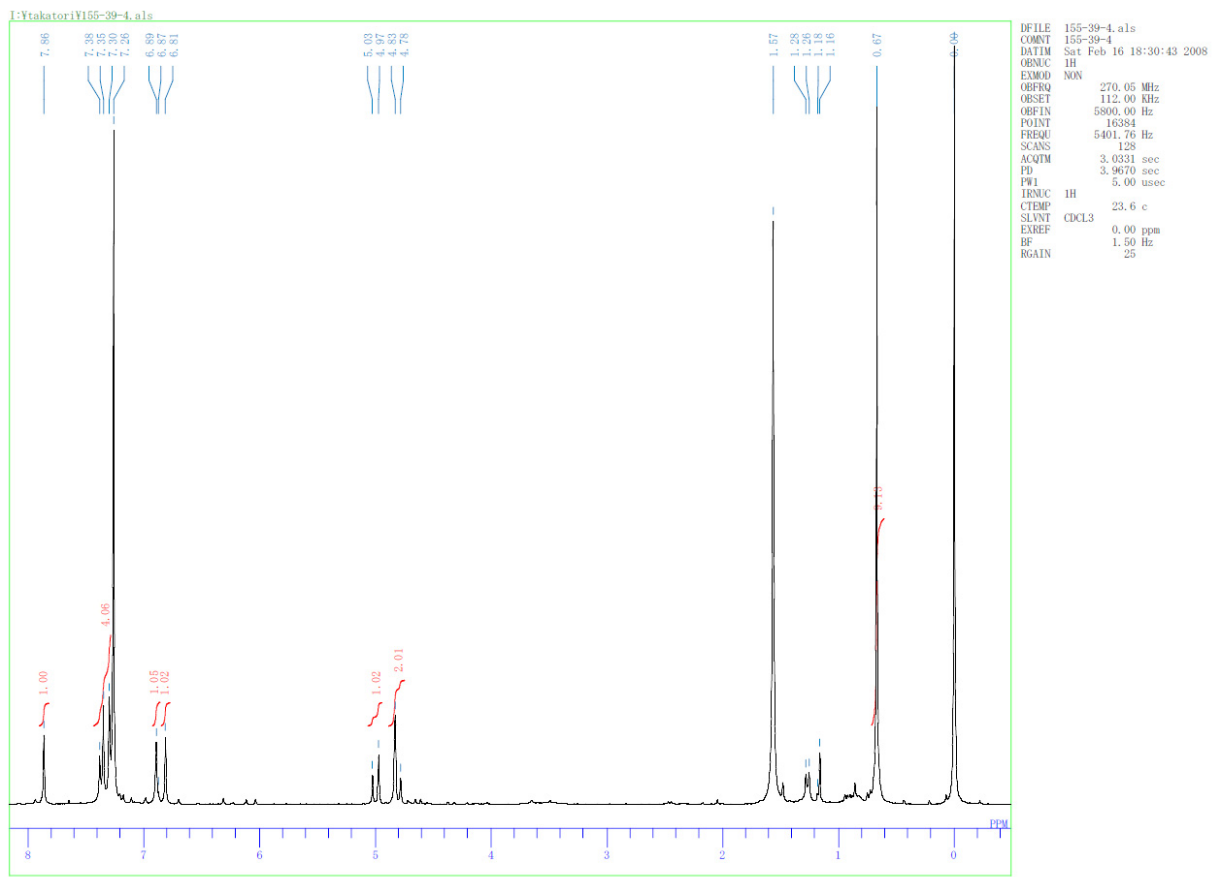
Compound *S*-9
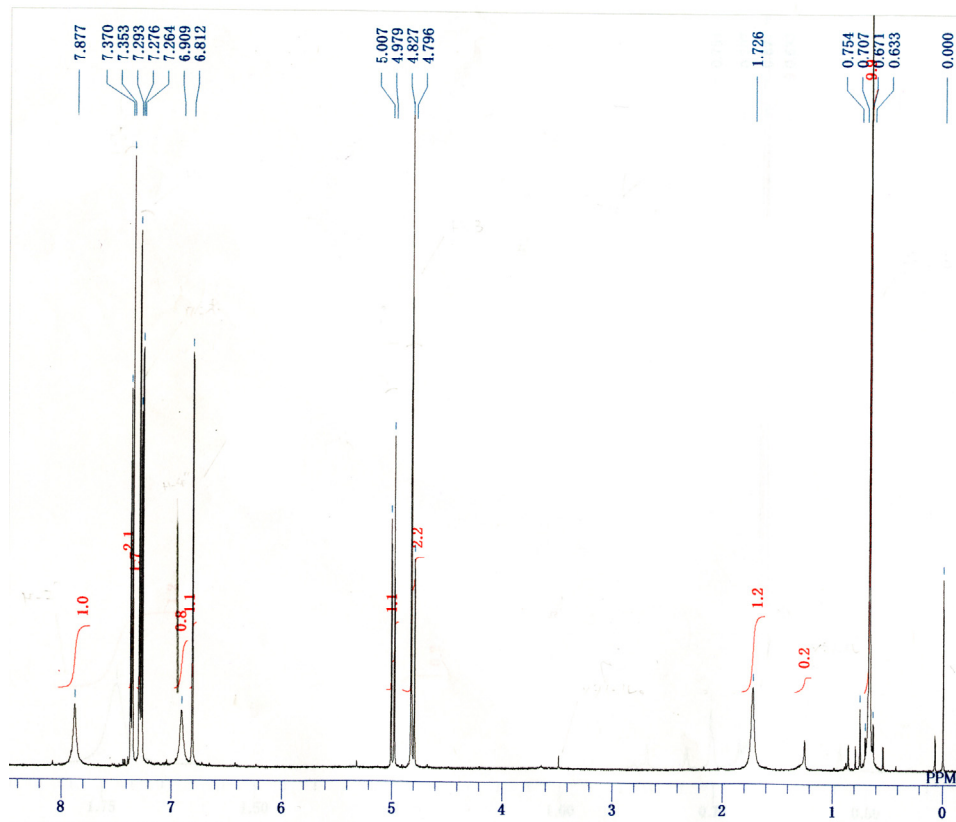
DFILE	A167172-h.als
COMNT	167-17-2
DATIM	Thu Jul 17 17:31:08 2008
OBNUC	1H
EXMOD	non
OBFRQ	500.00 MHz
OBSET	0.00 KHz
OBFIN	162160.00 Hz
POINT	32768
FREQU	10000.00 Hz
SCANS	16
ACQTM	3.2768 sec
PD	6.1810 sec
PW1	2.95 usec
IRNUC	1H
CTEMP	28.1 c
SLVNT	CDCL3
EXREF	0.00 ppm
BF	0.12 Hz
RGAIN	20

Compound *R*-9
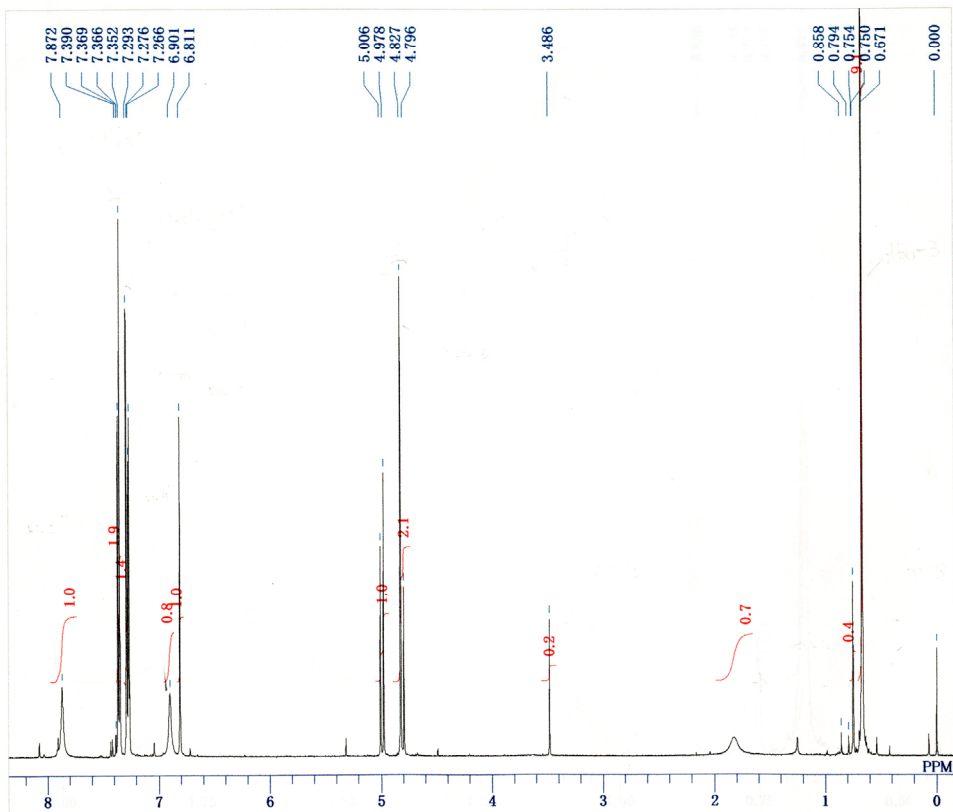
DFILE	167233-h.als
COMNT	167-23-3
DATIM	Tue Jul 22 13:51:18 2008
OBNUC	1H
EXMOD	non
OBFRQ	500.00 MHz
OBSET	0.00 KHz
OBFIN	162160.00 Hz
POINT	32768
FREQU	10000.00 Hz
SCANS	16
ACQTM	3.2768 sec
PD	6.1810 sec
PW1	2.95 usec
IRNUC	1H
CTEMP	28.1 c
SLVNT	CDCL3
EXREF	0.00 ppm
BF	0.12 Hz
RGAIN	20

13